8 Inertial confinement fusion: laser

[W.J. Hogan]

8.1 Introduction

Sections 5.3.3 and 5.5 above introduced the reader to the principles of inertial fusion power plant design and technology requirements. This chapter will explore the development of laser fusion technology in more detail.

Solid state lasers have dominated driver selection in research facilities whose main purpose was to study the physics of inertial fusion targets. These lasers, when focused to a small spot, are able to obtain the very large energy density necessary to study target physics even at small laser size and cost. Small solid state lasers [90Low, 92Bas] like Janus and Argus were used with small-scale hohlraums similar to that shown in Fig. 5.9a or with direct drive targets similar to Fig. 5.9b to demonstrate fundamental principles underlying inertial fusion. Early direct drive experiments [64Bas, 72Nuc, 85CEL, 98Lin] showed that fuel capsules containing DT fuel could be compressed and heated to produce a burst of thermonuclear reactions . Early indirect drive experiments showed that small hohlraums could be heated from the inside by well-focused laser beams and produce uniform high temperatures (several tens of eV) surrounding the fuel capsule. They also showed that the X-rays produced in these hohlraums could compress and heat DT fuel capsules to extremely high density and produce a small, central hot spot that, if the target were larger, might ignite a radially propagating thermonuclear burn front.

The ability to do substantive target physics work with relatively small solid state lasers led to a succession of facilities that advanced the state of the art in laser science and technology and in understanding of the physics of both direct and indirect drive targets. Figure 8.1a shows a succession of such lasers built at the Lawrence Livermore National Laboratory while Fig. 8.1b shows the energy and power attained in each laser pulse. All of these lasers were based upon using Nd-doped glass pumped with flashlamps as the laser amplification medium. The National Ignition Facility (NIF) laser main amplifier module [94NIF], shown in Fig. 8.2, is an example. In the figure one can see a 2×4 array of amplifier glass slabs flanked by vertical flash lamps. The flashlamps are filled with xenon gas which efficiently turns an electrical pulse into broad-band light. This light excites the Nd^{3+} ions in the glass. These excited ions emit 1.06 μm photons when stimulated with a seed pulse of the same wavelength. The eight 40 cm square laser beams come through the glass slabs at Brewster's angle out of the drawing. Gas would travel in the vertical direction between rows of flashlamps to cool the glass slabs and the flashlamps between pulses. This amplifier architecture works well because the fluorescence lifetime of the excited state of Nd in glass is relatively long (of order ms) compared with the pulse length of the seed pulse (of order ns). Therefore the flashlamps could be pumped with long duration power pulses and the laser light extracted in short times, greatly multiplying the power on target. As an example, the Nova laser pulse contained only 40 kJ of energy, but when this energy was compressed into 1 ns the power in the target was 40 TW, more than 100 times the total electric power generated in the United States. Furthermore when the laser focused on a small spot (order 10 μm) it produced a power density of more than 10^{14}…10^{16} W/cm^2 for a nanosecond. This was more than enough to produce hohlraum temperatures in Nova experiments of more than 100 eV [86Kau].

With each increase in size, there were significant advances in laser science and technology. These advances kept the cost of each larger facility to a manageable level. The decreasing cost per Joule of laser light shown in Fig. 8.3 made it possible to proceed much faster in laser energy on target than the increase in budget for each facility would have otherwise allowed.

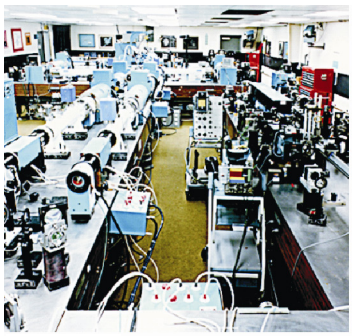

Janus (1974)

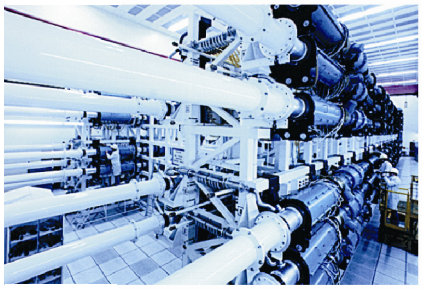

Shiva (1977)

Nova (1984)

a

Argus (1976)

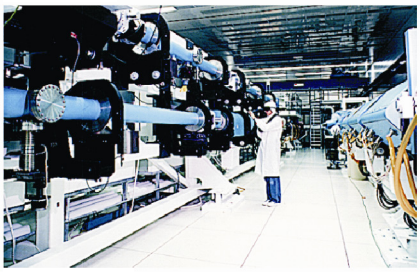

Novette (1983)

Beamlet-NIF prototype beamline (1994)

b

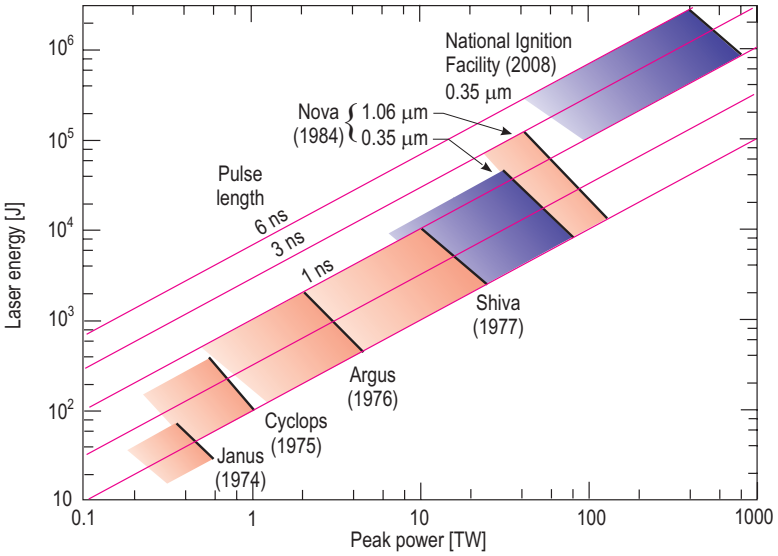

Fig. 8.1. **(a)** A succession of flashlamp-pumped Nd:glass lasers was built at LLNL for target physics research. **(b)** Each succeeding laser had more total energy and power in its pulse.

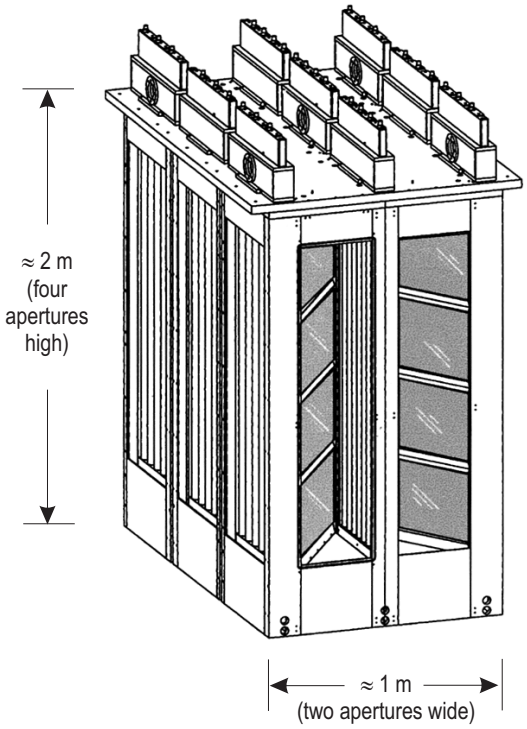

Fig. 8.2. An amplifier module of the NIF laser demonstrates the basic laser architecture of the flashlamp-pumped solid-state laser. Laser glass slabs for eight square aperture beams may be seen, flanked by flashlamps. The eight beams would come out of the drawing while gas would flow vertically between flashlamp rows to cool the glass between pulses.

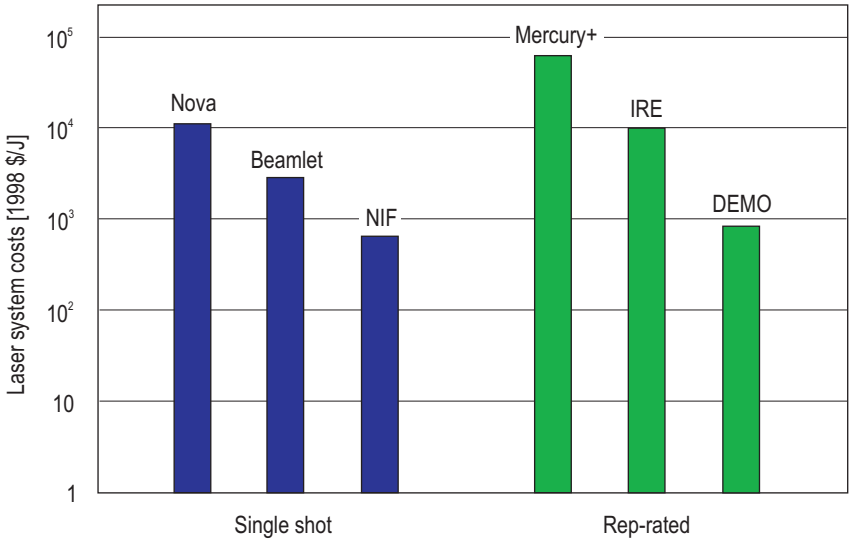

Fig. 8.3. Each successive laser built had a smaller cost per Joule contained in the laser pulse (IRE and DEMO are projections for diode-pumped solid state lasers of the future). This allowed larger solid state lasers to be built without a proportionately larger budget.

The culmination of this progression of solid state lasers is the construction of the NIF in the United States [04Mos] and the Laser MegaJoule (LMJ) in France [04Cav]. Figure 8.4 shows a schematic of the NIF, constructed in Livermore CA. It will deliver 10 ns pulses of more than 1.8 MJ of energy at 0.35 μm wavelength and a power of about 500 TW. It is expected that this will allow ignition of inertial fusion targets and an energy gain of about a factor of ten (i.e. the thermonuclear energy produced will be ten times the energy of the laser pulses put onto the target). Already the NIF has turned on four of its planned

192 beamlines. Figure 8.5 shows the architecture of one of these beamlines. A seed pulse of about 10 J in 10 ns is injected at the focal point of a spatial filter and expanded to the full 40 cm square aperture of NIF. The pulse goes through both amplifiers and hits a deformable mirror that removes phase front errors. When the pulse goes through the Pockels cell switch its polarization is rotated 90º so that the mirror that injected it into the amplifier cavity is now transparent. The pulse hits the flat mirror and is sent on a second round trip through the amplifier cavity. Again its polarization is rotated and then the switch is turned off so that the pulse is now reflected out of the main amplifier cavity. It then goes through the booster amplifier and is sent to the final optics which change the wavelength to 350 nm by frequency tripling in a non-linear optical material and focus the beam onto the target. The major difference from previous flashlamp-pumped Nd:glass lasers is that the pulse traverses the main amplifier four times rather than once to increase the efficiency. This set of four beams has performed better than the specifications by producing more than 40 kJ of 0.35 µm light in the four laser pulses (as much as the ten-beam Nova laser) [04Gle].

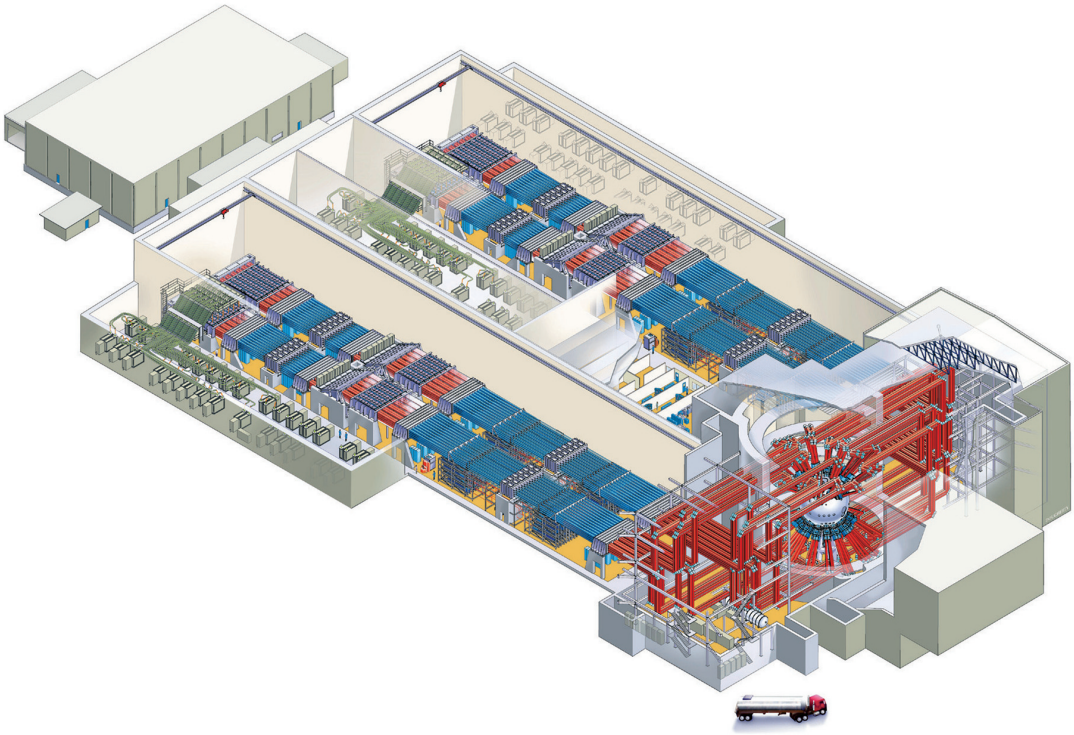

Fig. 8.4. The NIF laser is an example of the largest flashlamp-pumped Nd:glass laser built to date.

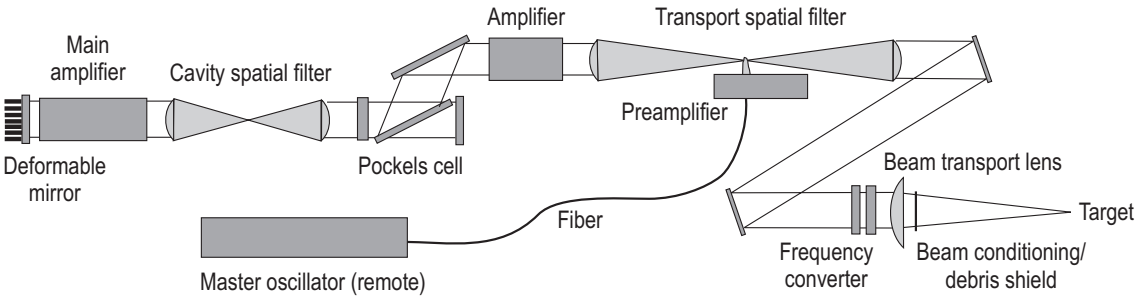

Fig. 8.5. Architecture of one beamline of NIF.

The demonstration of ignition and significant target energy gain will be the scientific proof of principle needed for the development of IFE. Gains of one to ten on NIF will show that the central hot spot has ignited a radially propagating thermonuclear burn front and that it has propagated a significant distance in cold compressed fuel. For IFE targets it will remain to demonstrate larger target gains by compressing larger masses of fuel and to show that this process can be repeated several times per second.

In spite of their success and widespread use in inertial fusion target physics research facilities, the flashlamp-pumped Nd:glass laser cannot be developed into an acceptable driver for IFE power plants. This is because these lasers are not well suited to repetition rates of several Hz and their efficiency is too low. The pulse rate is difficult to achieve because a great deal of heat is deposited in the laser glass with each shot and it is difficult to thermally cycle quickly without unacceptable stress fracturing of the glass itself. As was shown in Sect. 5.5, a desirable driver efficiency is of order 10 %. The overall efficiency of the NIF laser is about 1 % [94NIF]. This is about as high as one can go with flashlamp pumping. Flashlamps convert electrical energy into very broad band light, only a tiny fraction of which is absorbed into the excited state of the Nd ions embedded in the glass.

Two types of lasers are considered by most to be frontrunners for an IFE laser driver: the KrF gas laser and the diode-pumped solid state laser. They both have the potential to achieve the required efficiency, repetition rate and other requirements for a power plant. They will each be described in more detail in the following sections. In addition, the following sections will discuss the combination of target types, reaction chambers and other development subsystems that pair most beneficially with laser drivers. Finally, the possible development paths and issues for laser fusion will be discussed.

8.2 Target types most suitable for laser drivers

Section 5.5 described the basic central-ignition direct and indirect drive targets as well as the more recently introduced fast-ignition targets. In principle, any of these targets can be used for laser fusion. However, for several reasons the community has focused upon central ignition direct drive targets and dry walled chambers for laser fusion. This position results from several issues. First, fast ignition has, until recently, been considered very speculative and unproven (many still consider it so). Therefore the focus has been on central ignition targets. The quest for indirect drive ignition with these targets has led to the conclusion that symmetric capsule implosion in a laser-driven hohlraum requires a large number of beams with an illumination geometry that subtends a large solid angle. For example, the beam geometry for central ignition indirect drive targets of the NIF is shown in Fig. 8.6. Each end of the hohlraum must be illuminated with 96 beams, eight beams are needed for azimuthal symmetry, and both small and large angles of incidence in each ring must be used at each end in order to produce a uniform bath of X-rays throughout the implosion duration. At the chamber wall, this illumination geometry begins to look strikingly like that required for direct drive. Thus, chamber designs like the thick liquid designs like HYLIFE II shown in Sect. 5.5 may not be possible for laser drivers with these targets. Furthermore, the likelihood of achieving the uniformity necessary for direct drive increasingly appears possible as researchers have improved the smoothness and energy balance of beams shinning directly on the fuel capsule. Finally, gain calculations on a self-consistent basis indicate that at any given drive energy direct drive targets will give a higher gain than indirect drive ones. Therefore, the laser fusion design community has, in recent years, concentrated on direct drive central ignition targets and compatible chamber designs for laser drivers.

A wedge of a typical fuel capsule from an indirect drive ignition target is shown in Fig. 8.6c along with the temporally shaped laser pulse required to drive it to ignition. Note that this figure shows both the laser power and the hohlraum temperature as a function of time.

For direct drive targets on NIF, 12 quads (48 beams) are relocated to the equatorial region of NIF to illuminate the target uniformly from all directions. A section of a typical central ignition direct drive target [02Se] is shown in Fig. 8.7. Also shown is the temporally shaped laser pulse needed to drive it. It consists of a central gaseous DT region that will become the ignition hot spot, a liquid or solid layer of DT fuel, a layer of liquid DT fuel in a foam matrix that will act as the ablator for compressing the fuel and heating the hot spot to ignition, and a very thin layer of high-Z material (in this case, 500 Å of Pd) that helps to reduce the imprint of laser intensity inhomogeneities that could lead to hydrodynamic instabilities.

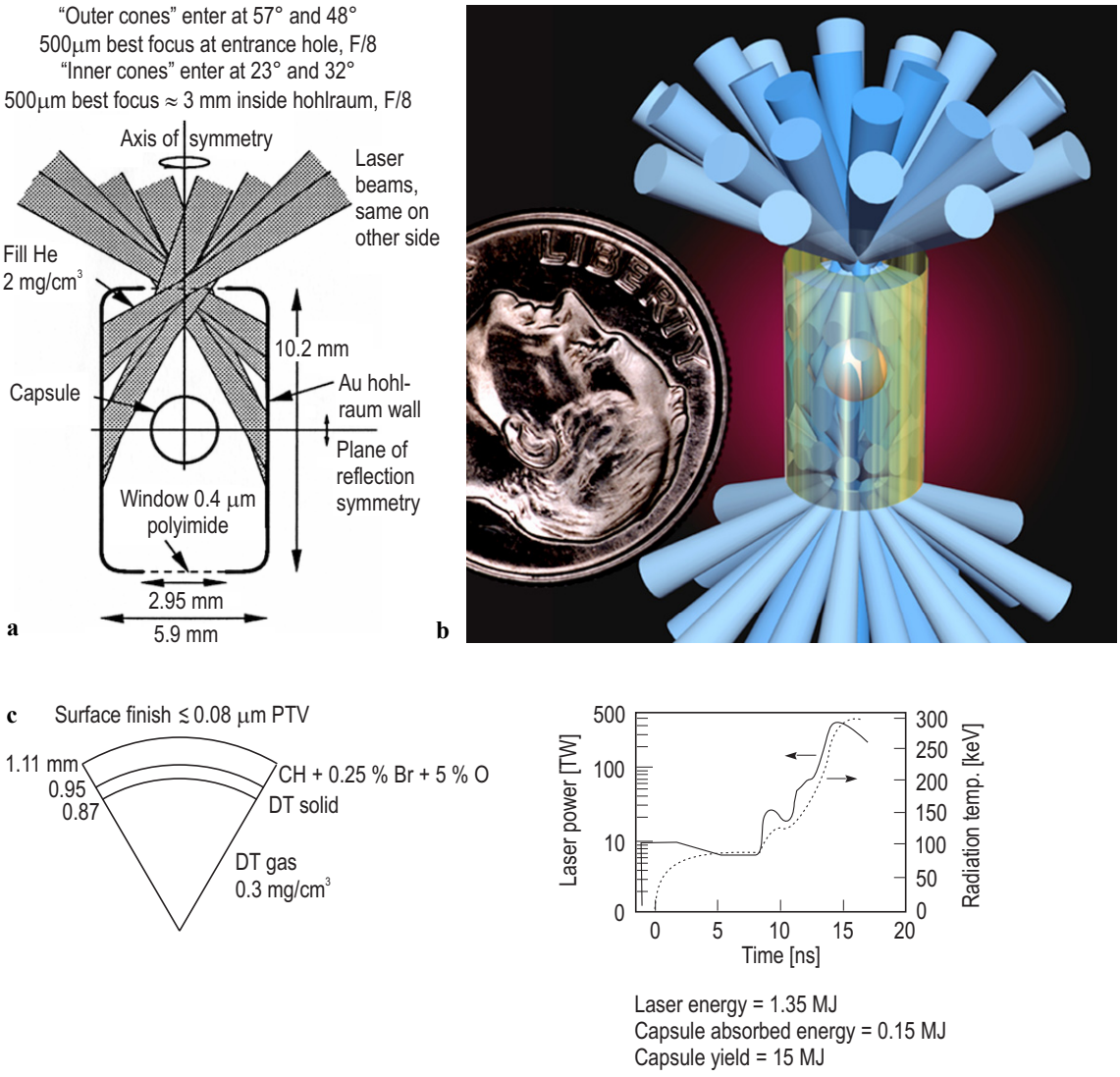

Fig. 8.6. The illumination geometry built for the NIF involves a symmetric array of 192 beamlines: **(a)** details of the illumination of one end of a hohlraum; **(b)** a scale artist's rendition of the whole target illuminated from both ends with a US ten cent piece shown for size comparison; **(c)** a wedge of the fuel capsule for a NIF ignition capsule along with the temporal pulse shape required to drive the target to ignition.

The critical questions for direct drive targets have been whether the beams can be made smooth enough spatially and whether the balance of energy and power among the beams can be accurate enough that target symmetry requirements are met. Progress through a variety of innovative techniques (to be discussed in the laser sections below) has been rapid and now most in the laser fusion community believe these goals can be met.

As pointed out in Sect. 5.5 fast ignition targets decouple the implosion and ignition stages in such a way that the total driver energy to obtain high gain may be much smaller than that required for central ignition targets. Also noted in Sect. 5.5 is that it was widely recognized that the major uncertainty in the concept was whether the ignitor beams could penetrate the plasma blown off the fuel capsule during the implosion phase. In the last few years a newer concept called "cone focus" fast ignition targets and experiments on these have raised expectations that these targets may work. Figure 8.8 shows the configuration of two cone focus targets, one a direct drive and the other an indirect drive target [04Hog]. The purpose of the high atomic number cone is to shield the line of sight of the ignitor beams from the expanding

plasma. The cone may also protect the target during injection and make it less vulnerable to turbulence in the chamber [03Nor]. Experiments have shown that the presence of the cone significantly enhances the thermonuclear reactions produced by the ignitor beams [01Kod]. Besides giving larger gains at lower driver energy, fast ignition targets may be less demanding on the uniformity of illumination required of the driver. This is because the compression phase simply has to get a blob of fuel to a density of a few hundred g/cm^3. It does not have to form a central hot spot that must ignite. The latter task results in the stringent uniformity requirements of the central ignition targets, whether direct or indirect drive. Relaxing the uniformity requirement may allow laser drivers to use indirect drive targets effectively. Thus for the fast ignition concept, both direct and indirect drive targets should be considered.

The fuel capsules for fast ignition targets are similar to those of central ignition shown in the above two figures with a few differences. First, of course, the cone is added. (Direct-drive fast-ignition targets may not have a cone but the coupling efficiency of such a target is in doubt so only cone focus targets will be considered here.) The cone is a high-Z material that protects the ignitor beam line of sight from the expanding plasma. When a high atomic number cone is added to the direct drive target it will behave, during target handling processes, more like a hohlraum target. The cone must be thick enough not to break up during the implosion of the fuel capsule attached to it. As an upper limit consider 50 Mbar pressure for 15 ns duration. Not allowing the cone to move more than one thickness would require a thickness of about 260 μm of Pb (realistically the cone could move several thicknesses before breakup). It must be long enough that the plasma blow-off from the capsule does not get into the line of sight of the ignitor beams. These conservative assumptions lead to a cone length of about 4 times the radius of the fuel capsule. This cone would weigh about 0.3 g, i.e. about the same weight as a typical hohlraum.

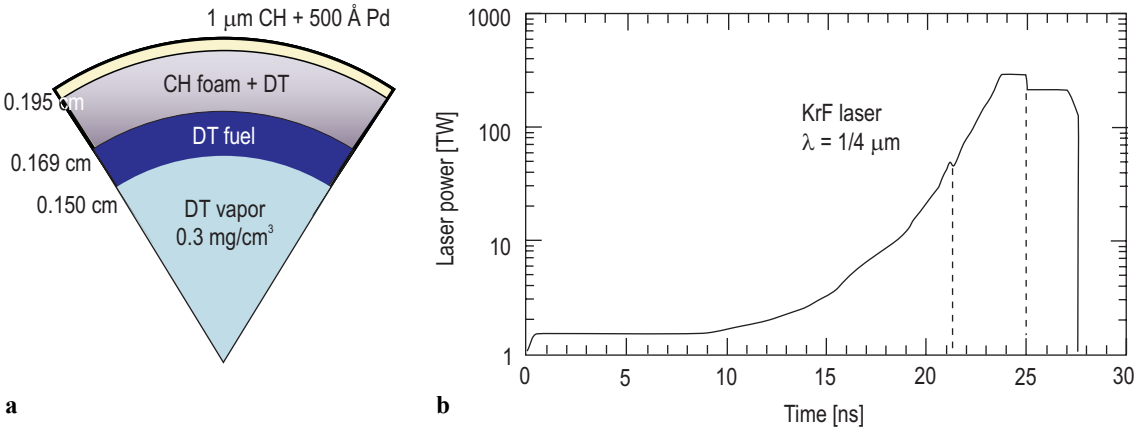

Fig. 8.7. **(a)** A wedge of a typical central-ignition direct drive target. **(b)** The temporally shaped laser pulse needed to drive it to ignition. The dashed lines show when aperture "zooming" should occur to efficiently use the laser energy.

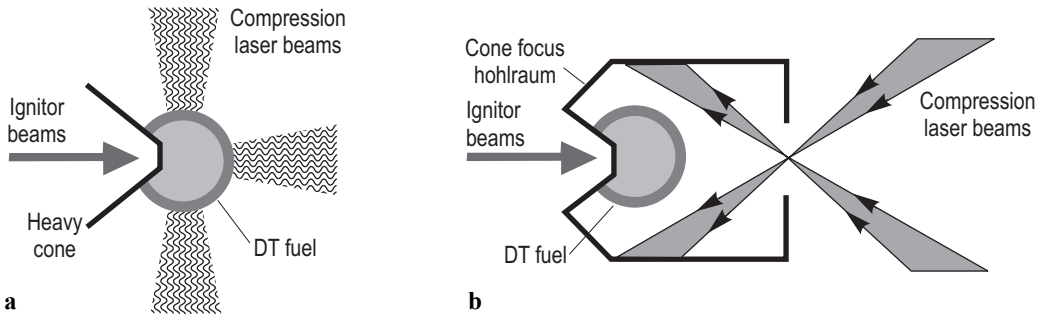

Fig. 8.8. Designs of laser-driven cone focus fast ignition targets: **(a)** is for direct drive, and **(b)** is for indirect drive.

On the other hand, when adding a cone to a hohlraum, the cone need only be long enough to connect to the hohlraum, i.e. about twice the radius of the fuel capsule. This is because the plasma is retarded by the hohlraum. Thus, with the exception of aerodynamic stability upon injection, the direct and indirect drive cone focus targets behave similarly during target handling processes.

For the direct drive cone target the outer Pd layer may not be necessary because of the reduced implosion symmetry requirements. The capsule for the indirect drive cone focus target is identical to that for a central ignition indirect drive target except that the surface finish on the capsule does not have to be so fine.

As was pointed out in Sect. 5.5, a major goal of target design is to find a target that will give sufficient gain at the lowest driver energy (assuming only that cost decreases with decreasing driver energy). Figure 8.9 shows relatively recently calculated gain curves for laser-driven targets of various types [98Key]. Included are central ignition direct and indirect drive targets and fast ignition targets with various ignition conditions.

The figure shows two sets of indirect drive curves with different implosion velocities but only one set of direct drive curves. Nevertheless it can be seen that in general, above the ignition cut-off, direct drive can produce a larger gain than indirect drive. The figure also shows the potentially large advantage of fast ignition. For any reasonable assumptions about ignition condition, sufficiently high gain is produced at a much smaller driver energy than for either kind of centrally ignited target. This may allow inertial fusion power plants to be competitive at smaller plant size. There are, of course, still many power plant issues to be solved for any kind of laser target. However this set of gain curves shows that there are many reasonable approaches for laser fusion.

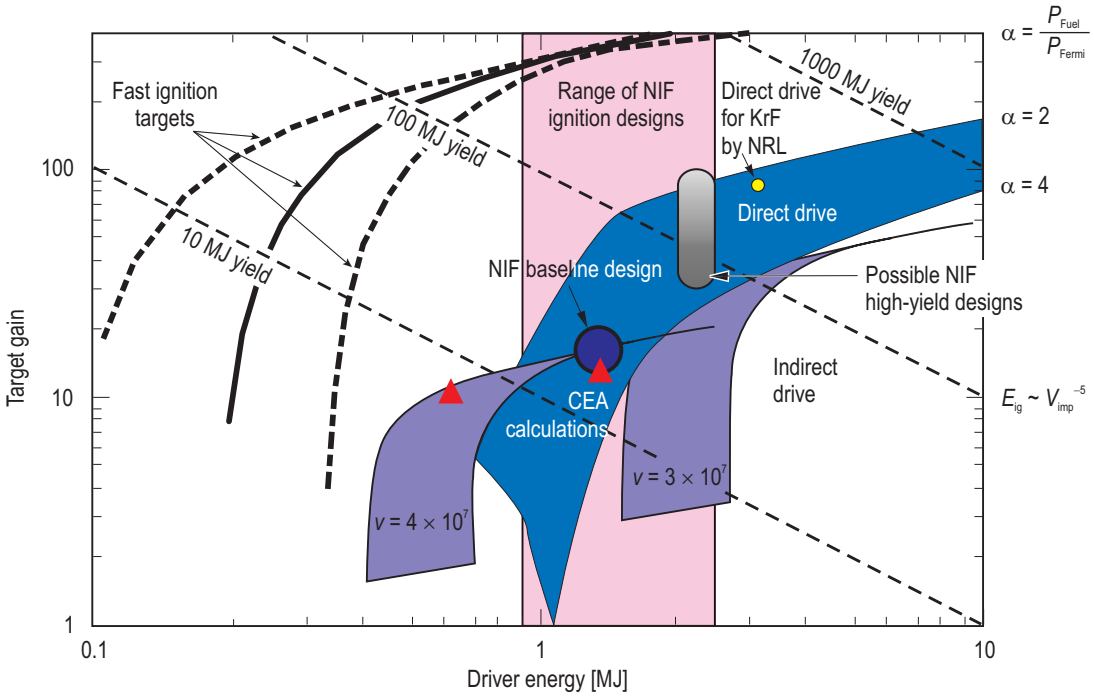

Fig. 8.9. Gain curves for various laser-driven targets and conditions.The bands represent estimated known uncertainties in the calculations.

8.3 Laser drivers: KrF, solid state

As noted in Sect. 5.5.3 the first requirement for an inertial fusion driver is achieving the extremely high intensities and small spot sizes necessary to compress and heat small quantities of thermonuclear fuel. It is the natural ability of lasers to satisfy these requirements that makes them the preferred driver for target physics facilities worldwide, as noted above, and also makes them contenders as power plant drivers. The key to their success in this role is their ability to meet the other driver requirements, in particular high average power (through repetition rates of 1…10 Hz), high efficiency (7…10 %, dependent on gain), durability and cost. Many types of lasers have been considered and several types experimented with for this purpose. The two leading laser candidates at present are the KrF laser and the diode-pumped solid state laser (DPSSL). The next sections will describe these lasers.

8.3.1 KrF lasers

KrF lasers are one of the two leading laser driver candidates for several reasons. Their 248 nm wavelength increases the rocket efficiency of the fuel capsule compression and raises the threshold for deleterious laser-plasma instabilities. They have excellent spatial uniformity, have the capability to "zoom" (decrease the spot size to match the compressing target size, thereby increasing the coupling efficiency), and they are modular so that a small module can be built and tested and then replicated for the full-scale driver. Development programs are underway in Japan [99Oku, 01Oku], China [02Wan], Russia [01Zvo], and the United States [03Set1, 04Set]. Much of the material of this section is extracted from [03Set1, 04Set] and from discussions with the author of these references.

KrF is an excimer laser based on a molecular electronic transition to a ground state. It uses a combination of the gases krypton, fluorine and argon (used as a buffer) at 1…2 atmospheres as the laser amplifying medium. While the fundamental wavelength is 248 nm, there are many rotational and vibrational transitions so KrF lasers have a very large bandwidth (1…3 THz). Small KrF lasers are pumped with a discharge. Electron beams are used to pump fusion-sized laser systems (10 J to 10s of kJ, pulses of 20…100 ns). Figure 8.10 shows a basic module of a repetitively pulsed, electron beam pumped KrF laser driver. It consists of a laser cell that contains the gases, two opposed electron beam systems, a foil structure to separate the gases in the laser cell from the vacuum of the electron beam system, and a laser gas recirculation system. The electron beams pump the laser gas at right angles to the laser propagation direction and the gas recirculation system operates in the third direction, as shown in the figure. For each pulse, the electron beams are fired to create the excited KrF state. Then an input laser pulse at 248 nm wavelength is amplified by extracting the excitation energy. Normally the laser beam would be reflected back through the laser cell in a "double pass" arrangement to increase laser efficiency. For simplicity, this is not shown in Fig. 8.10.

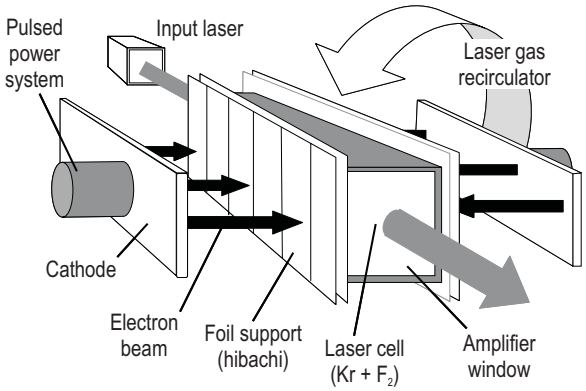

Fig. 8.10. Components of a basic KrF laser module.

From beam stopping considerations the electron beam voltage ranges from 500 to 800 keV and currents in the range of 100 to 500 kA. The laser gas pressure and the electron beam parameters are adjusted to achieve uniform energy deposition across the cell. An external magnetic field prevents the electron beam from pinching as it propagates into the laser cell. KrF amplifiers have been built without a magnetic field, however those with the field have proven to be more efficient and are more compatible with the gas recirculator [04Set].

Between pulses the laser gases must be cooled and "quieted", i.e. returned to their full pre-excitation condition. Most of the electron beam energy will end up as heat and other excited states, since the maximum "intrinsic" efficiency (ratio of energy extracted in the KrF laser beam to the energy deposited by the electron beams) envisioned is 12 %. The purpose of the laser gas recirculator system is to de-excite and cool the gas to prepare it for the next pulse.

8.3.1.1 Timescale issues

The (KrF)* excited state has a spontaneous relaxation time of 7 ns. To contain the correct energy needed for exciting the laser gas mixture using reasonable pulsed power systems, the electron beams will have durations of several hundred nanoseconds. These timescale inconsistencies are reconciled by the following means. A seed pulse of the correct duration and pulse shape for the target implosion is created at the beginning of the laser path. This seed pulse is replicated many times and, through angular multiplexing, these seed pulses are passed sequentially through the amplifier for the entire pump duration. Thus the laser light is continually extracted during the entire electron beam pulse. Then the series of amplified short pulses are restacked, again using angular multiplexing, at the target so that the proper pulse length and intensity is seen by the target.

8.3.1.2 Beam smoothing

Direct drive targets require that the laser beams impinging upon the capsule surface have very good spatial uniformity. Non-uniformities in the beam intensity cause perturbations that grow due to hydrodynamic instabilities. This non-uniform growth could ultimately prevent ignition of the central hot spot or even break up the capsule before sufficient compression occurs for efficient burn. Therefore, as pointed out in Sect. 5.5, the spatial variation in the laser intensity on target must be less than 1 %.

One advantage of KrF lasers is that they have a large bandwidth due to the large number of rotational and vibrational lines available to the lasing molecules. The large bandwidth of KrF enables one to use the spatial and temporal incoherence to produce very uniform illumination of the target. The instantaneous target illumination profile of a KrF beam has the speckle pattern characteristic of all spatially multimode lasers. However, the large bandwidth causes this speckle to change on a timescale that is short compared to the response time of the target. However, it was observed that the initial non-uniformities in the beam can be a problem. These first non-uniformities can "imprint" a pattern on the capsule surface that can produce seeds for instability growth.Therefore, a variety of additional techniques for reducing intensity variations has been investigated and successfully employed. These include random phase plates [84Kat, 89Sku], smoothing by spectral dispersion [89Sku], and induced spatial incoherence (ISI) [87Leh1, 87Leh2].

At NRL only the ISI technique is used and this has been found to be sufficient. In the ISI technique several laser pulses are artificially "offset" in time so that they are essentially incoherent when they reach the target. An aperture is illuminated with this incoherent broad-band laser light and is imaged through the laser system and focused onto the target, as shown in Fig. 8.11. The Nike laser at the Naval Research Laboratory in the United States has demonstrated this technique and has produced a very uniform focal profile. The rms speckle uniformity in each laser beam was on the order of 0.3…1.3 % [96Obe]. This very high uniformity reduces the imprinting (or seed) of modulations on a fusion target, and, hence, mitigates the growth of hydrodynamic instabilities.

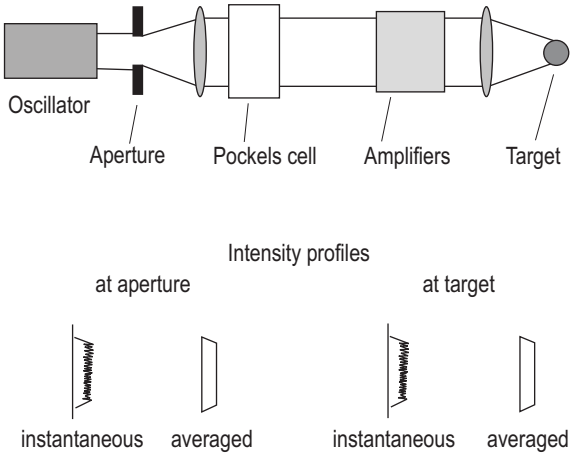

Fig. 8.11. **(a)** Optical train of a KrF laser, and **(b)** intensity profiles at different locations.

8.3.1.3 Pulse shaping and zooming

It was noted in Sect. 5.5 that the target would like to see a temporally shaped pulse with a low "foot" and a rising intensity profile such as that shown in Fig. 8.7b above. The foot raises the isentrope of the ablator which lowers its susceptibility to hydrodynamic instabilities. Sometimes there is a "prepulse" added to reduce the growth of hydrodynamic instabilities. This works by spreading the abrupt density change at surfaces into a gradient in density that does not allow as much growth of various instabilities.

Zooming the driver beams is also desirable since with a constant diameter beam, more of the energy in the beam will miss the target as the target compresses. Both zooming and pulse shaping are achievable in a KrF laser.

Pulse shaping can be achieved in a KrF laser by adding a Pockels cell after the aperture to modulate the light (see Fig. 8.11). Zooming can be accomplished because the final pulse is made up of the smaller packets of pulses (described in Sect. 8.3.1.1 above). Parallel optical tracks are added to the seed laser with each track having its own unique sized aperture and a Pockels cell. By sequentially running the laser beam through smaller and smaller apertures, the laser spot size is decreased. One candidate target design has three zooming steps [00Bod]. Figure 8.7b shows the times (dashed lines) at which a three-step zooming process should occur during an idealized pulse shape.

8.3.1.4 Electron beam propagation and energy deposition efficiency

Large-area electron beam diodes are known to be subject to the "Transit Time Instability". The diode acts like a parallel plate microwave cavity and allows RF waves to propagate back and forth, resulting in the instability. The instability has been successfully modeled with the Mission Research Corporation (MRC) MAGIC particle-in-cell (PIC) code [03Fri1] and observed in experiments at the Naval Research Laboratory [04Set]. The instability imparts an axial velocity spread to the electron beam, which both lowers the electron beam energy that is deposited into the gas, and increases the amount of energy deposited into the "hibachi" foils. The PIC modeling showed the instability could be mitigated by precisely slotting the electron beam emitter (cathode) and loading the slots with microwave absorbing material [03Fri2]. The slots and absorbers turn the diode into a slow wave structure that impedes the RF waves from propagating at their natural frequency. Figure 8.12 shows the results of experiments on the Nike 60 cm amplifier [04Set]. The upper half shows the initial configuration, with a monolithic cathode. The plot shows the measured fast Fourier transform of the rate of change of current (dI/dt). The dominant peak at 2.5 GHz is in agreement with modeling. The lower half shows the slotted cathode (with microwave absorbers inserted into the vertical slots) and the resulting experimental Fourier transform of dI/dt. Note the amplitude of the instability is reduced by a factor of 40 000, i.e. it is effectively quenched.

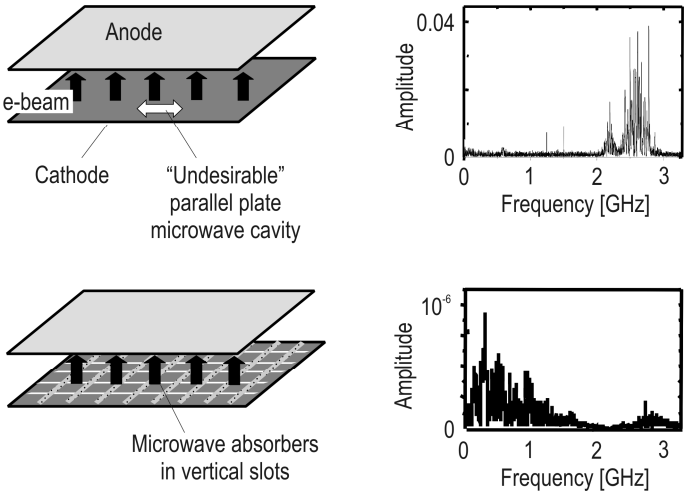

Fig. 8.12. A cathode configuration that eliminates the "Transit Time Instability" is shown below along with the fast Fourier transform. The slotted cathode completely eliminated the instability. Note the expanded scale on the lower transform.

Measurements at NRL with a stacked-foil energy spectrum analyzer agree with the modeling prediction that the resulting electron beam is close to mono-energetic, and therefore should deposit its energy in the gas in a uniform, predictable manner [04Set].

Another issue with the electron beam pumping is the efficiency. A thin foil separates the laser gas mixture from the vacuum region of the electron beam. A structure called a "hibachi" supports this foil with ribs so that the foil can be thinner. The hibachi must be as transparent as possible to the electron beam, in order to maximize the electron deposition into the gas. It must also be able to withstand the static pressure from the laser gas and the cyclic hydrodynamic shocks induced as the electron beam deposits its energy into the gas. The foil itself must be damage resistant to electrons, X-rays, ultraviolet (UV) light, and fluorine, and have a low reflectivity in the UV in order to prevent unwanted ASE transverse to the main optical axis. The US program in KrF lasers is examining titanium or stainless steel. High transmission requires not only that the foil be as transparent as possible to electrons, but also that the laser gas composition and pressure be adjusted to minimize back-scattered electrons.

NRL has developed a hibachi concept that demonstrates energy deposition transmission efficiency of 73 % on Electra (500 keV, 1 mil Ti pressure foil) [04Set, 04Heg]. This is in contrast to other large systems in which the efficiency is around 35…40 % [97Set]. The energy deposition efficiency is the ratio of the energy deposited in the laser gas divided by the electrical energy in the diode. The energy deposition during the 100 ns flat top portion of the electron beam pulse are considered in this analysis. The high transmission efficiency was achieved with two innovations: (1) eliminating the anode foil that is customarily placed on the diode side of the hibachi structure, and (2) patterning the electron emitter into strips so the beam "misses" the hibachi ribs. While conceptually simple these are difficult in practice because the beam strips spread due to the highly non-uniform electric fields caused by eliminating the anode foil, and they rotate and shear due to the beam's interaction with the applied magnetic field. To compensate for these the emitters are narrowed and "counter-rotated" so the beam strips propagate parallel to the ribs when they get to the hibachi. The concept is shown in Fig. 8.13.

Note that slotting the cathode into strips also eliminates the "transit time" instability as described above. While the topology of the strips can be determined empirically, this does not give us the predictive capability needed to design larger systems. This is a rather complex phenomenon to model and requires a full 3-D PIC simulation of the exact experimental geometry, including the rib structure, laser gas, and magnetic field. This was achieved with the Large Scale Plasma (LSP) code developed by MRC, Albuquerque. The simulations accurately predict both the cathode counter rotation angle and the energy deposition efficiency. The electron beam depicted in Fig. 8.13 is an LSP simulation of a beam "strip". The field shapers shown in the figure are used to reduce the current density enhancement that would normally occur at the edge of an electron beam [02Heg].

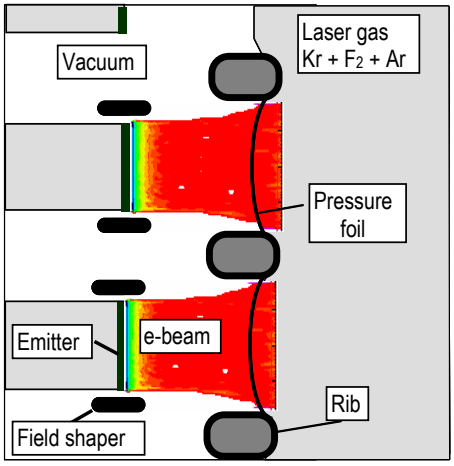

Fig. 8.13. High-efficiency hibachi and emitter configuration for KrF lasers.

8.3.1.5 Advanced pulsed power development

A pulsed power system that addresses IFE requirements for rep-rate (5 Hz), durability ($> 3 \times 10^8$ shots), efficiency (85 %), and cost ($8.50/pulsed power Joule) has been designed by NRL [02Wei]. It is a full-scale, 100 kJ (electrical) IFE-sized pulsed power system based on a Laser Gated and Pumped Thyristor (LGPT). The system would produce a 800 kV, 180 kA, 600 ns flat-top electron beam. The switch would be packaged in a rail gap configuration and be the basis for a low-inductance, ultra-fast Marx generator. The Marx would pulse charge a 600 ns pulse forming line, which in turn would be discharged by a single magnetic switch into a 600 ns transit time isolator (TTI) to drive the electron beam diode. The TTI minimizes the rise and fall times of the pulse.

The LGPT is based on an all-new, four-layer, solid-state switch that is optically triggered by two on-board diode laser arrays. The lasers flood the entire switch volume with photons to yield switching times of less than 100 ns. The lasers are kept on during the entire electrical current pulse to minimize the forward voltage drop and hence maximize efficiency. In first tests, an off-the-shelf four-junction thyristor was modified to accommodate a single diode laser array and its optical coupling. The switch operated at 3.2 kV for 10^5 shots at 5 Hz. The current density was 2.7 kA/cm^2 (121 % of the IFE system requirement) and the current rate of rise was 1.4×10^{10} A/(scm^2) (154 % of the IFE requirement). A second-generation switch that uses advanced, purpose-built construction techniques, including both anode and cathode gating arrays, has also been built. This switch will operate at the full IFE-required operating voltage of 16.8 keV. A schematic of this switch appears in the upper half of Fig. 8.14 while the schematic of the entire pulsed power system appears in the lower half.

8.3.1.6 Gas recirculation system

A gas recirculation system has been designed to cool and quiet the laser gas between shots, and to cool the hibachi foils [04Set]. This is achieved by installing a set of moveable airfoils, or louvers, just upstream of the laser cell. The louvers are parallel to the gas flow, to ensure a uniform laser gas just before the electron beam fires. This uniformity is essential for high-quality laser focal profiles. Immediately after the electron beam pulse the louvers are rotated sideways to block all but a few cm of the 30 cm wide gas flow channel. This trips the gas into turbulence and removes heat from the foils. After 100 ms, the louvers are fully opened, which gives ample time for the gas to return to a quiescent state for the next shot. The first tests of this on the Electra system at NRL have demonstrated that the foils can be cooled with this technique [04Set, 04Heg]. Figure 8.15 shows the foil temperature (as measured with a thermocouple) for three different conditions with the system operated at 1 Hz. The working gas was argon and thus there was no laser in these tests. Note that with no cooling at all, the foil temperature reached 360 °C, whereas with the gas flowing and the louvers actuating, the foil temperature lowered to 140 °C. There have been 1250 shots continuous at 1 Hz, with no degradation in the foil.

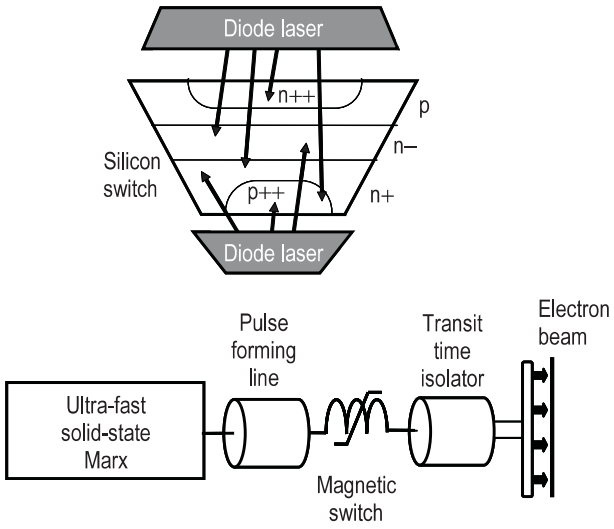

Fig. 8.14. Schematic of a 100 kJ pulsed power system suitable for an IFE-sized beam. It uses the LGPT (shown above the pulsed power schematic) in an ultra-fast Marx generator.

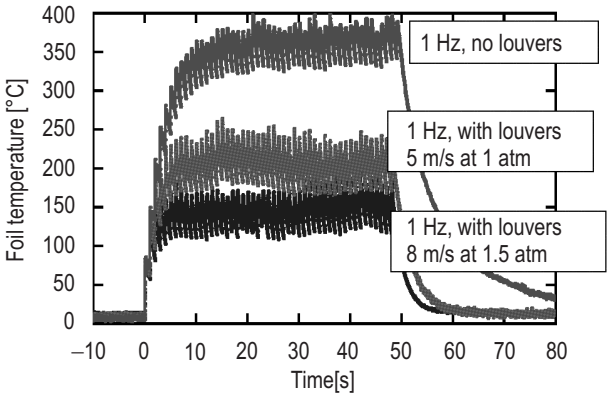

Fig. 8.15. Foil temperature under various conditions of laser gas velocity and with or without louvers.

8.3.1.7 Platforms for KrF laser research and development

KrF laser research at NRL is carried out with two facilities. Electra is a repetitively pulsed facility that has produced 500 J of laser light as an oscillator. Presently, the electron beams are powered by a "First Generation" pulsed power system that is capable of continuously operating at 5 Hz for 100000 shots [00Set]. While this system does not meet the IFE requirements for durability and efficiency, it provides a durable pulsed power platform to develop the laser components. The Electra facility produces two counter-propagating electron beams, each of energy 500 keV, current 100 kA, flat top pulse width 100 ns, and area 27 cm × 97 cm. Electron beam runs consisting of 10000 shots or more are routine with this system. While Electra is sufficient to develop the laser technologies, there are some issues with the electron beam physics that must be investigated on a larger electron beam diode. These are carried out with the Nike laser 60 cm amplifier, which produces opposing 750 keV, 500 kA, 240 ns, 60 cm × 200 cm electron beams [97Set]. A full-scale fusion energy beam line would have an array of electron beam diodes, and each of those diodes would be the same size, or slightly smaller than the Nike diode.

8.3.1.8 System efficiency

Electra has been operated as an oscillator. The laser cell is 30 cm wide (between pressure foils) by 30 cm high, by 100 cm long (along the laser axis). The laser resonator was created by adding a flat 98.5 % reflecting rear mirror and an 8 % reflecting output coupler. The required output coupler reflectivity was determined using the well-established Rigrod formula [65Rig]. The laser gas pressure was varied between

1.0 and 2.0 atmospheres, with various concentrations of fluorine, krypton, and argon. The maximum laser energy was observed at fluorine concentrations of 0.25 %. At lower concentrations there is insufficient fluorine to allow maximum lasing throughout the pulse (the so-called "fluorine burn-up"), whereas at higher concentrations the excess fluorine absorbs the laser light. The laser output increases with increasing total pressure, because the electron beam deposition increases with pressure. However, the maximum laser output occurs at a pressure that is below that needed to fully stop the electron beam in the laser cell. This occurs because deleterious three-body interactions become more important at the higher pressures. The laser output is also larger at lower krypton concentrations because the three-body interactions are more severe with krypton than argon. The maximum laser output was found to be 510 J. In this case the electron beam pump was 700 kW/cm^3, the laser gas pressure was 20 psi, and the gas composition was 39.75 % Kr, 60.0 % Ar, and 0.25 % F [04Wol].

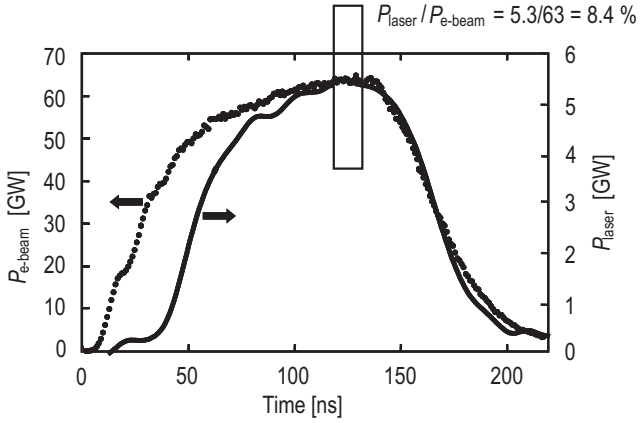

Fig. 8.16. Laser "intrinsic" efficiency of Electra operating as an oscillator.

Of particular importance to an IFE system is the intrinsic efficiency of a KrF system. Figure 8.16 shows the laser output pulse superimposed on the electron beam pump pulse for Electra operating as an oscillator [84Kat]. The electron beam power is determined by the pressure rise in the gas after the electron beam deposits its energy, and allowing another 10 % for radiation. Note that at the peak of the laser pulse, the observed intrinsic power efficiency is ≈ 8.4 %. This observed intrinsic efficiency is in very close agreement with previous investigations [80Ric] after accounting for the actual window transmission in the Electra experiments of 70…80 %. The efficiency of Electra as an amplifier is expected to be around 12 % because it will be run without an output coupler and the windows will have higher transmittance. In addition, an amplifier is intrinsically more efficient because it is not amplifying a very low input as occurs in the early times in an oscillator. In other words energy is not wasted to build up the gain.

Based on current research, the overall wall plug efficiency for an IFE-sized KrF system can be on the order of 7.5 %. The breakdown is shown in Table 8.1.

Table 8.1. Component efficiencies of an IFE-sized KrF system.

Component	Basis	Efficiency
Pulsed power	Advanced switch	87 %
Hibachi	No anode, pattern beam	80 %
KrF intrinsic	Electra experiments	12 %
Optics to target	Estimate	95 %
Ancillaries	Pumps, recirculator	95 %
	Total	7.5 %

8.3.2 Diode-pumped solid state lasers (DPSSL)

As described in Sect. 8.1, flashlamp-pumped Nd:glass lasers, while being the mainstay of inertial fusion research facilities to study target physics, are not suitable as an IFE driver because of their inefficiency and limited pulse rate capabilities. They are inefficient mainly because flashlamps emit extremely broad bandwidth light while the absorption band of the Nd^{3+} ion in the glass is very narrow. Therefore most of the flashlamp light ends up as heat in the glass rather than in excited ions. They have limited pulse repetition capability because glass is a good insulator and has poor thermal fracture toughness. When heat removal between pulses is attempted, large temperature gradients develop that stress the glass beyond its thermal fracture limit.

Diode-pumped crystalline lasers solve both these issues and, therefore, the diode-pumped solid state laser (DPSSL, pronounced "dipsel") has become one of the two leading candidates for an IFE laser driver. Laser diodes efficiently emit light in a very narrow bandwidth. If one can pick the emission frequency to coincide with the lasing ion's absorption frequency, a very efficient laser will result. Figure 8.17 shows the overlapping bands for one combination. In this example the emission spectrum of an InGaAs (indium-gallium-arsenide) laser diode is compared to the absorption spectrum of Yb:S-FAP (ytterbium-doped strontium fluorapatite, $Yb^{3+}:Sr_5(PO_4)_3F$) crystals. Since the laser diode efficiently converts electrical energy into light energy, a combination like that shown can have a high overall efficiency. Laser slope efficiencies (ratio of the increase in laser output energy to the increase in absorbed optical pump energy) of more than 50 % have been observed.

Crystals are good conductors of heat and can have acceptable fracture toughness. Therefore they can also satisfy the heat removal requirements for high repetition rate. The results of one set of experiments [95Pay] are shown in Fig. 8.18. The thermal flux from the laser slab is plotted against the repetition rate. For comparison a power plant point design [92Svi] is shown along with the allowed design region below which fracture is avoided.

Figure 8.19 shows a schematic of a possible DPSSL. The elements of this laser driver are an input pulse from an oscillator and preamplifier system, a main amplifier, a frequency conversion system, and a final focusing and standoff system. Frequency conversion is necessary because shorter wavelengths than are usual for solid state lasers are thought necessary to avoid laser-plasma instabilities that produce hot electrons that can cause poorer target performance. Most lase in the 1000 nm range while the target prefers less than 500 nm light.

The architecture in this schematic is similar to that of the Nd:glass research laser and, therefore, much that has been learned in development of those research tools can be applicable to the development of DPSSLs. Furthermore, the frequency conversion system can be similar to that employed in the Nd:glass research facility drivers. In those systems a combination of KDP and KD*P (potassium dihydrogen phosphate and the deuterated version of the same) crystals is used to double or triple the frequency to reduce the lasing frequency below 500 nm.

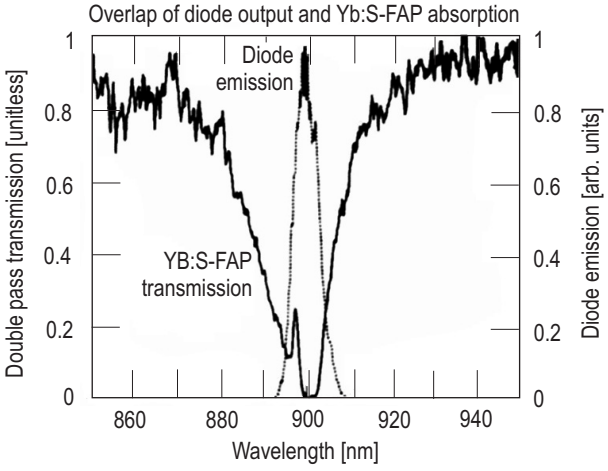

Fig. 8.17. Overlapping emission and absorption bands.

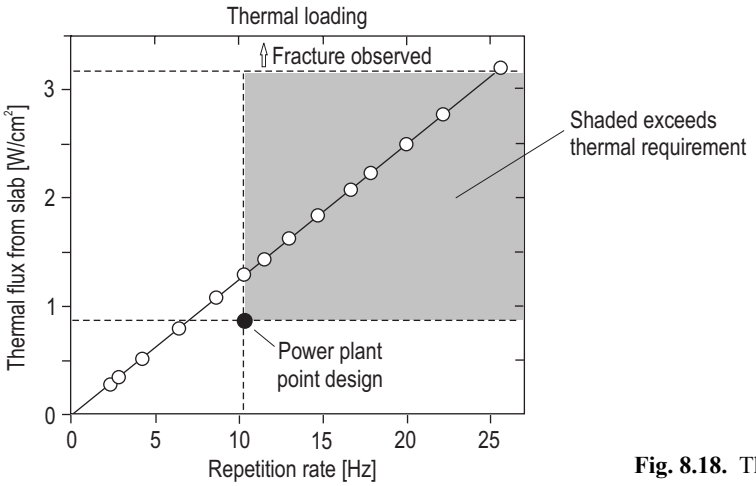

Fig. 8.18. Thermal fracture survival figure.

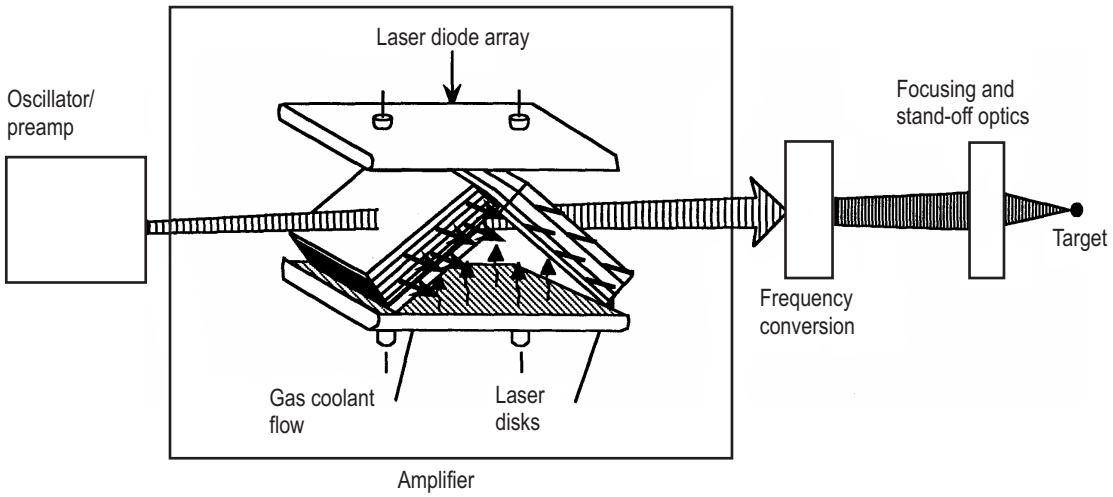

Fig. 8.19. Schematic of a DPSSL.

8.3.2.1 Timescale issues

To achieve high efficiency at low cost, DPSSLs must solve a timescale issue. Laser diodes efficiently convert electrical energy into light energy but are essentially CW devices. Figure 8.20 shows the results of experiments in Japan on laser diode arrays. The laser diode (LD) array power and the electrical to optical efficiency are shown as a function of the LD current. Efficiencies over 45 % were observed. On the other hand, the energy in the excited state of the lasing ion is be extracted on a timescale shorter than the emission lifetime of that excited state (< 10 ns to drive the target). Therefore, to take most advantage of the efficiency of laser diodes it would be desirable to find a lasing ion/host crystalline material that has a longer emission lifetime than that of Nd^{3+} used in Nd:glass lasers.

Measurements were made on phosphate glass and several crystals doped with either Nd or Yb. Figure 8.21 shows a map of the extraction cross section versus emission lifetime space for these combinations. There are limits to the operational space within this map. If the extraction cross section is too large, the system will be limited by amplified spontaneous emission (ASE). If it is too small the system will be limited by laser damage to the optical elements. The acceptable range is also shown in Fig. 8.21. The Yb:S-FAP combination results in the longest emission lifetime within the acceptable range of extraction cross section [95Kru].

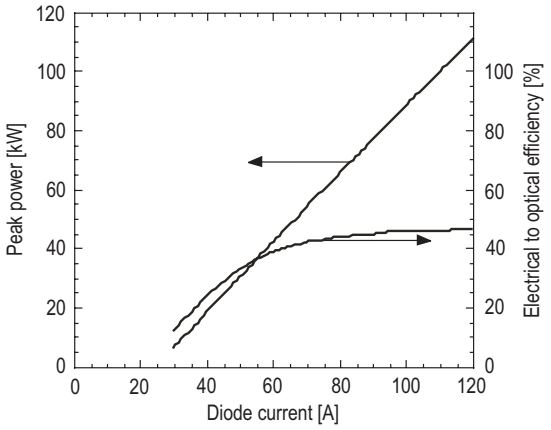

Fig. 8.20. Laser diode array efficiency from Japanese experiments (kindly provided by Dr. T. Kawashima of ILE, Osaka University).

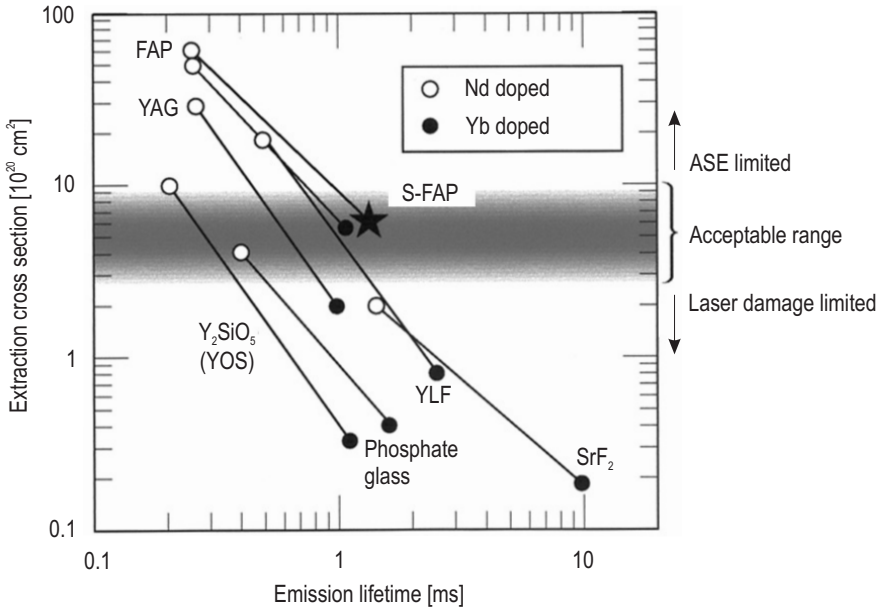

Fig. 8.21. Extraction cross section as a function of emission lifetime for several laser materials [95Kru].

8.3.2.2 Beam smoothing issues

In general many of the beam smoothing techniques described in Sect. 8.3.1.2 above for KrF lasers can be used for DPSSLs. However, in contrast to KrF lasers, the characteristic bandwidth for solid state lasers is inherently narrow. Furthermore, as the input pulse is amplified the bandwidth grows narrower. This would be a disadvantage for DPSSLs in attempting to achieve very uniform intensity profiles. However, techniques have been developed for increasing the effective bandwidth and for keeping it broad as the pulse is amplified.

Spectral sculpting [01Pay] can help keep the bandwidth broad as the pulse is amplified. If a spectrally flat pulse is input to the system, then the output is narrowed. However, if the pulse is sculpted, i.e. given higher intensity at the ends of the bandwidth, then the output pulse will be flat and without the amplitude modulations that would otherwise appear. Figure 8.22 shows the effect of this technique. Parts a and b show the output for a flat input pulse. The bandwidth is narrowed and contains amplitude modulations. Parts c and d show the resulting output if the input is spectrally sculpted in the manner described above. The resulting output is broad-band and has no amplitude modulations.

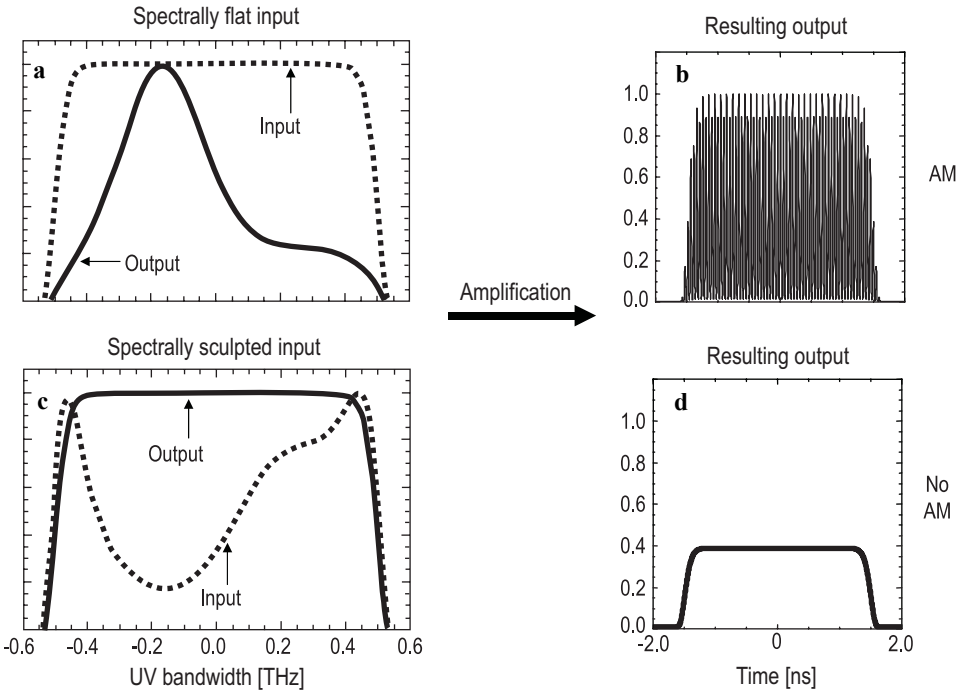

Fig. 8.22. Spectral sculpting can reduce amplitude modulations and keep the bandwidth broad on a DPSSL.

8.3.2.3 Two approaches to DPSSL design and development

In solid state lasers beam uniformity is better if care is taken to pump the laser slabs uniformly and to extract the heat from the slabs uniformly as well. These are more easily accomplished if the diode array light impinges normally on the laser slabs and the heat is extracted perpendicular to this direction. Nevertheless, there will still be gradients in the population of the excited state in the direction perpendicular to the large surface of the slabs. Therefore, while the amplifier schematic shown above in Fig. 8.19 could in principle be made to work, in fact the two major DPSSL development programs in the world are each taking a somewhat different approach to the design of the DPSSL and both are different from the schematic in Fig. 8.19.

The two centers for DPSSL work are the Lawrence Livermore National Laboratory (LLNL) in the United States and the Institute for Laser Engineering (ILE) at Osaka University in Japan. At LLNL scientists are pursuing a design in which the laser beams pass through the laser slabs normal to the large slab surface. The diode arrays also pump the slabs in the same direction. Excitation gradients are still produced but every part of the laser beam samples all parts of the gradient and, therefore, the beam remains uniform. Gas flows perpendicular to this direction in narrow channels between the slabs. This approach is shown in Fig. 8.23.

The Japanese approach is to use the zig-zag laser architecture [04Nak]. In this case the slabs are pumped normal to the large surface of the slabs as above but the laser beams are injected into the slabs through one of the narrow edges. As they travel through the length of the slab, the laser beams zig-zag back and forth between the surfaces by internal reflection. Therefore, again the beams sample all parts of the excitation gradient. This architecture is shown in Fig. 8.24.

The researchers in Japan are also examining different lasing materials [04Nak]. The lasing materials Yb:YAG and Nd:Y_2O_3 have a larger thermal shock parameter than Yb:S-FAP. They are examining making ceramic lasers because of their ease of fabrication and possibilities for low-cost mass production. They find that Nd:Y_2O_3 ceramic lasers can have broad-band and a thermal conductivity three times larger than YAG.

The two approaches to the DPSSL complement one another. Each has advantages and disadvantages compared to the other. Development of both approaches will allow the best to emerge naturally.

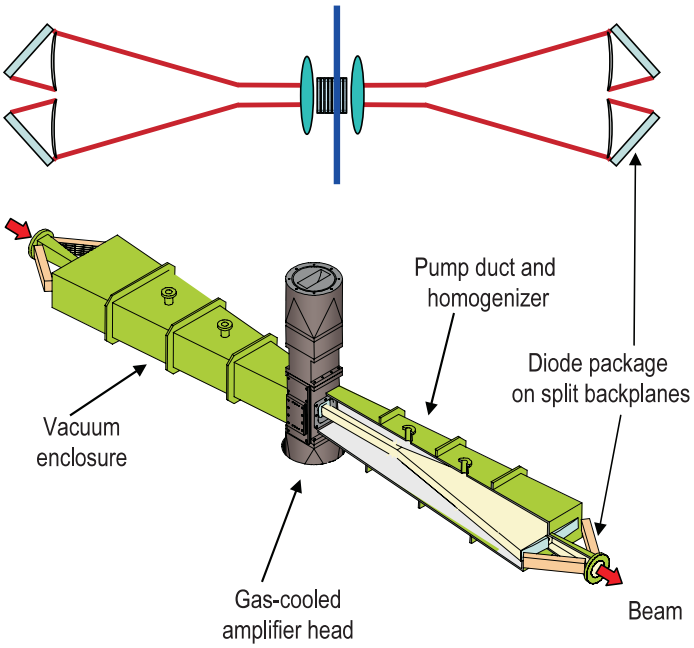

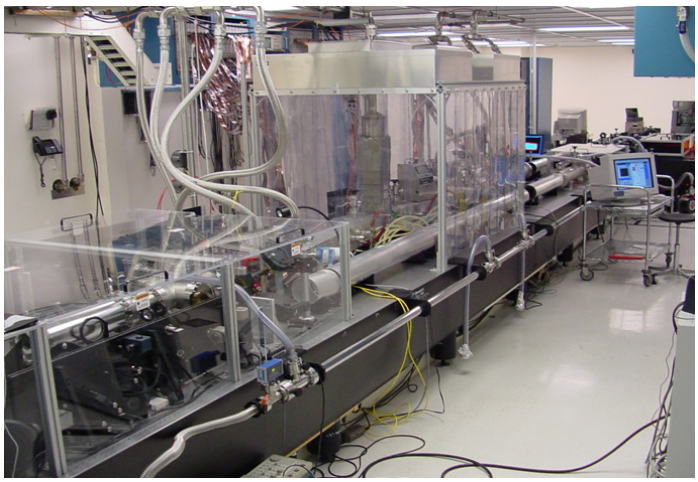

Fig. 8.23. **(a)** The split backplanes on which the diode arrays are mounted [01Pay]. The diode light is focused onto the amplifier head from the same direction as the path of the laser beam being amplified. **(b)** The amplifier enclosure. **(c)** The Mercury demonstration laser at LLNL.

8.3.2.4 Diode array development and cost reduction issues

Both approaches to the DPSSL laser require development of inexpensive laser diode arrays to pump the lasing medium efficiently. The V-BASIS packaging techniques of the LLNL approach [01Pay], shown in Fig. 8.25, illustrates the progress in this development. As shown in the figure, long thin diode bars are set into a V-notch in a silicone substrate. Microlenses, fabricated in a manner similar to fiber-optic cables, are placed along the thin, emitting side of the diode. These microlenses focus the diode light toward the laser slabs.

The array has been able to produce 120 W peak per cm of array with a 45 % efficiency in converting electrical energy into optical energy. The array has been run at 10 Hz and been reliable for $> 2 \times 10^8$ shots. The backplane shown in the above figure has operated at 10 Hz with an average power of 532 W [01Pay]. Figure 8.26 shows the emitted spectrum and temporal pulse. There was less than 5 % droop observed during the 0.7 ms pulse.

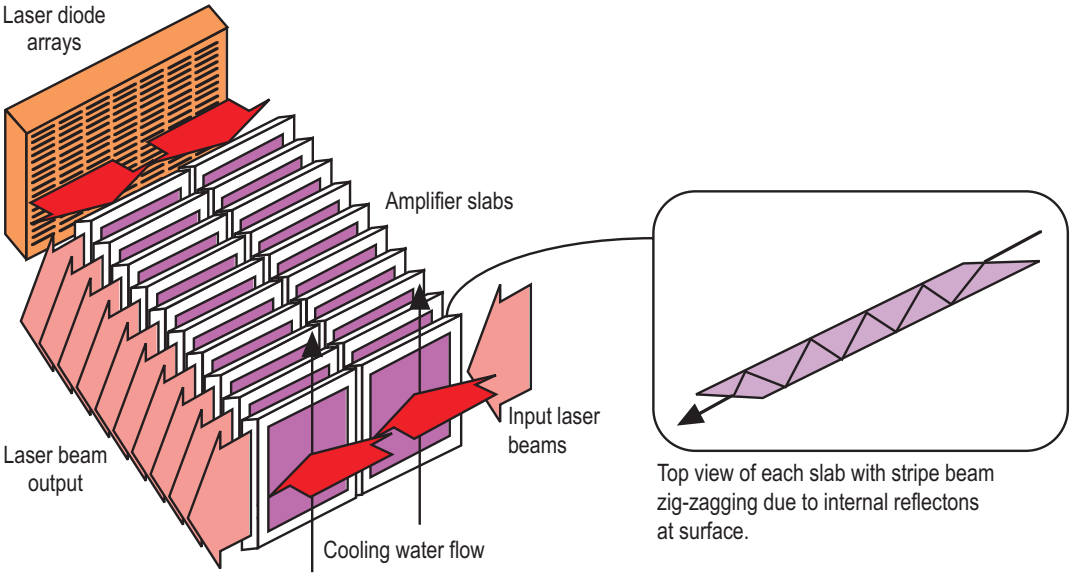

Fig. 8.24. In ILE's approach the laser beams zig-zag through the length of each laser slab (kindly provided by Dr. T. Kawashima of ILE, Osaka University).

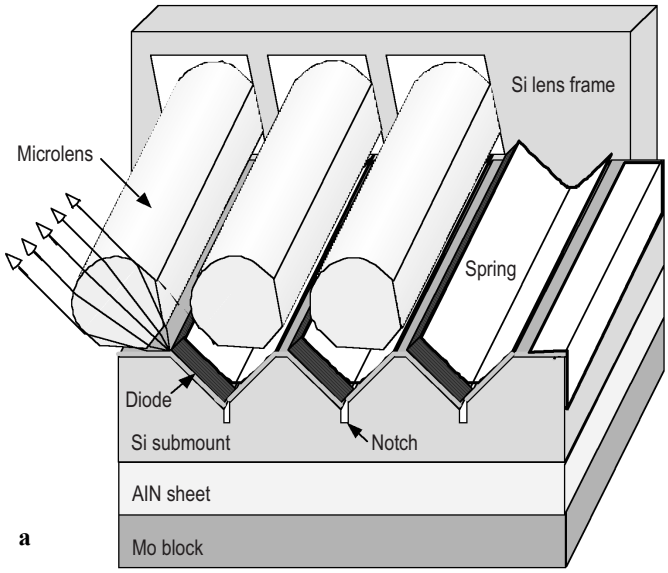

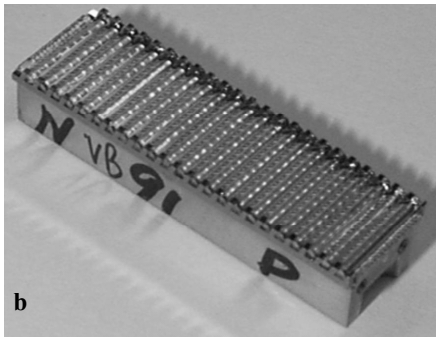

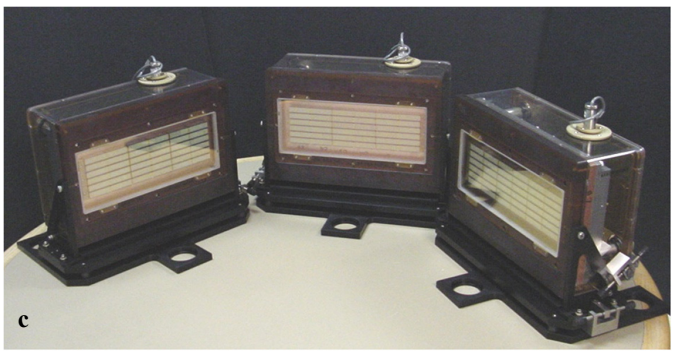

Fig. 8.25. The V-BASIS packaged diode bars meet the optical specifications. **(a)** Detail of the mounting scheme. **(b)** One slab of 25 mounted bars. **(c)** Three 6×6 arrays of such slabs each of which emits 80 kW (10 Hz, 1 ms pulses, 120 W/bar).

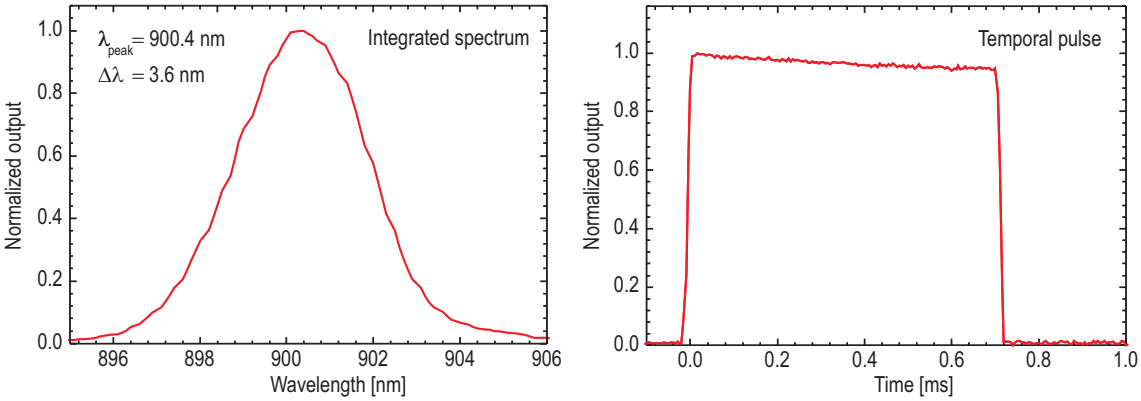

Fig. 8.26. The laser diode backplane demonstrated the desired spectrum and the constancy of the temporal profile [01Pay].

8.3.2.5 Laser medium growth

The LLNL team's near-term goal is to grow Yb:S-FAP crystals 3.4 cm in diameter and more than 6 cm long using the Czochralski method shown in Fig. 8.27. In this method, $SrHPO_4$, $SrCO_3$, SrF_2 and Yb_2O_3 compounds are melted by induction heaters. A seed crystal is then pulled from the crucible allowing the crystal to form as the seed is pulled. The boule is inspected and if it is acceptable, stresses are removed, the crystal is cut in half lengthwise and two 2 cm × 6 cm half slabs are fabricated as shown in Fig. 8.28. These half slabs are then joined to form one 4 cm × 6 cm full-size slab about 1 cm thick, as shown on the right side of Fig. 8.28.

The ceramic laser approach for crystals such as YAG forms and sinters the laser slabs from nano-crystals. Several groups in Japan are working on the development of such lasers. One group [01Lu] has reported a laser output of almost 1.5 kW from a ceramic YAG laser pumped with 3.5 kW from a laser diode array. The output of this laser is shown in Fig. 8.29.

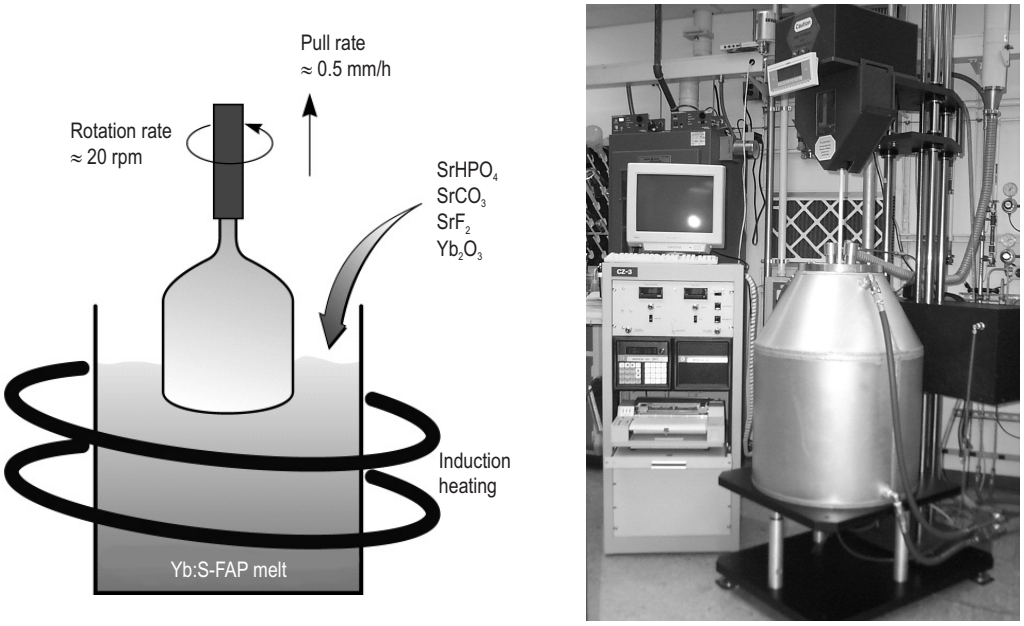

Fig. 8.27. Crystals of Yb:S-FAP are grown by using the Czochralski method [01Pay].

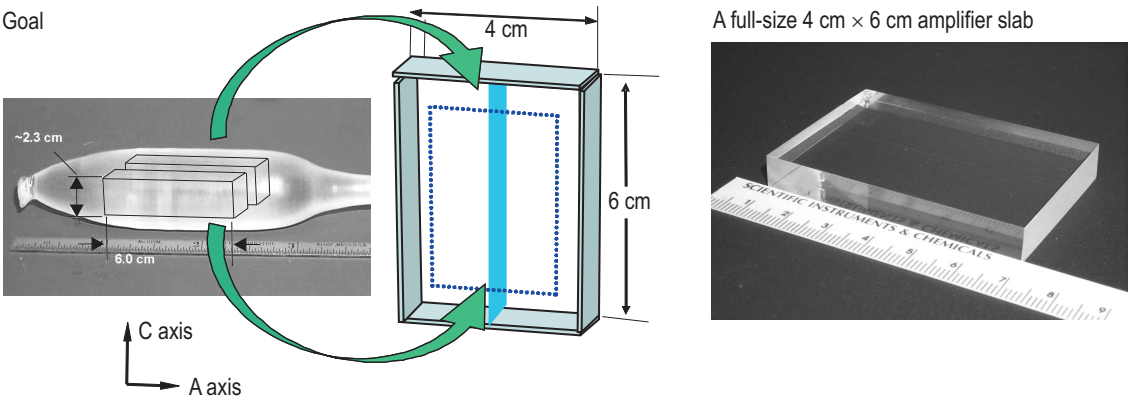

Fig. 8.28. Two half slabs are fabricated from the crystal boule and joined by diffusion bonding to form the full-sized crystal on the right [01Pay].

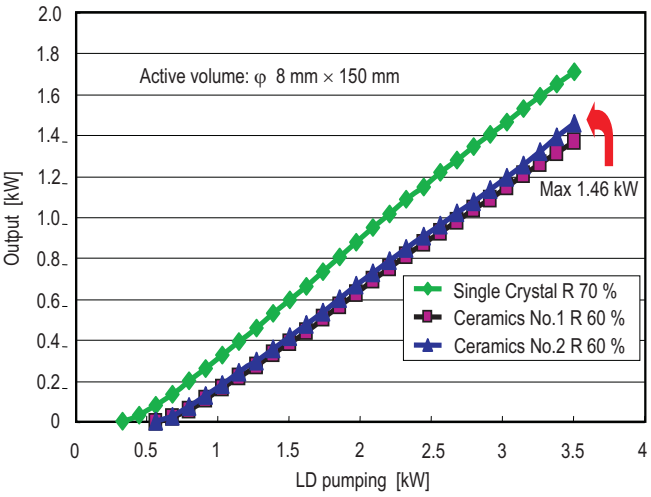

Fig. 8.29. A ceramic YAG laser pumped by a diode array has output almost 1.5 kW of power (kindly provided by Dr. T. Kawashima of ILE, Osaka University).

8.3.2.6 Repetition rate and amplifier cooling issues

Both approaches to the DPSSL must be actively cooled to restore the laser slabs to the original condition between pulses. In the LLNL approach, He gas flows between the slabs in the stack and extracts heat from the crystals. An example of such cooling is shown in Fig. 8.30a for the LLNL approach. It should be noted that there will be a temperature gradient in the slabs in the direction of the flowing gas. Such a gradient will cause some bending of the laser beam. The laser slabs can be slightly wedged as in Fig. 8.30b to compensate for this effect. The complete amplifier head is shown in Fig. 8.30c.

8.3.2.7 Test beds for DPSLL development

The LLNL team is constructing the Mercury laser at LLNL to provide an integrated test of all the principles of their approach to the DPSLL. In the schematic of Fig. 8.31 one can see two amplifiers of the type shown in Fig. 8.23 above. The beam traverses each amplifier four times in order to extract a large fraction of the excited energy available. The beam is injected at the output end, travels through both amplifiers and is reflected from a deformable mirror that will remove phase front errors. The beam then travels through each amplifier a second time. Slight angular differences cause the beam to miss the injection mirror on the way out and instead hit the first mirror of the reverser. The reverser's function is to reinject

the beam into the amplifiers for another round trip. The Pockels cell in the reverser assures that parasitics do not arise in the amplifiers. These techniques for multipassing are similar to those used on the NIF laser described above.

The Japanese are constructing the HALNA laser to test the principles of the DPSSL approach they are taking [04Nak]. Figure 8.32 shows an artist's drawing of the HALNA zig-zag laser. This laser is also multipassed through the main amplifier gain media. In HALNA the slabs are Nd:glass and are water-cooled. The researchers plan to expand the laser in steps to demonstrate scalability to a full-size DPSSL driver for IFE as shown on the right-hand side of the figure.

Both groups plan to expand their facilities in phases. Figure 8.33 shows the current plans of each organization to develop full-scale IFE drivers by the end of the second decade of the 21st century [04Nak]. The time chart also shows past developments of solid-state research lasers through the NIF and LMJ facilities that plan to demonstrate ignition within the next decade.

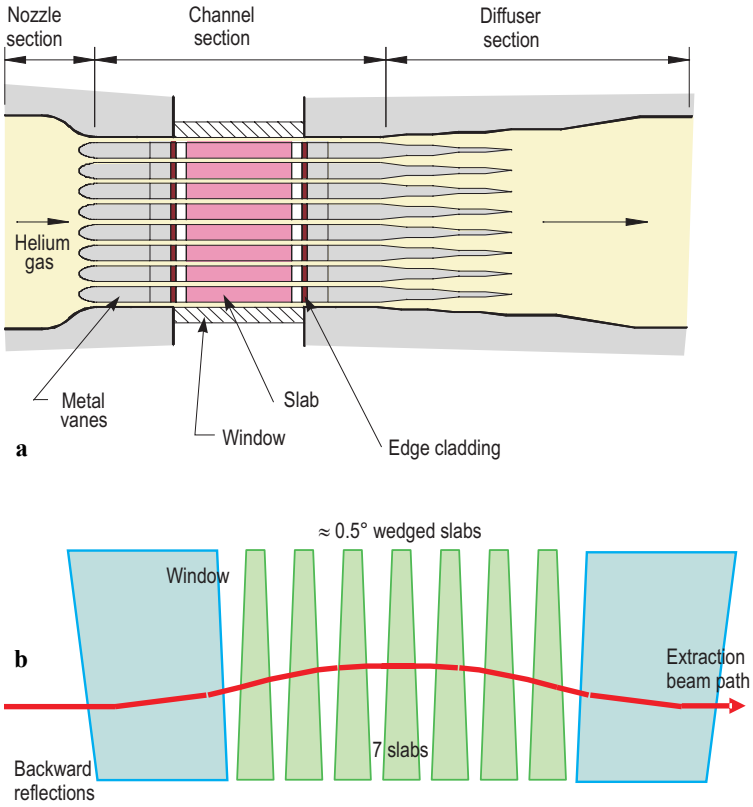

Fig. 8.30. **(a)** The laser slabs in the LLNL approach are cooled with flowing He gas. **(b)** The laser slabs can be slightly wedged. **(c)** A complete amplifier head [01Pay].

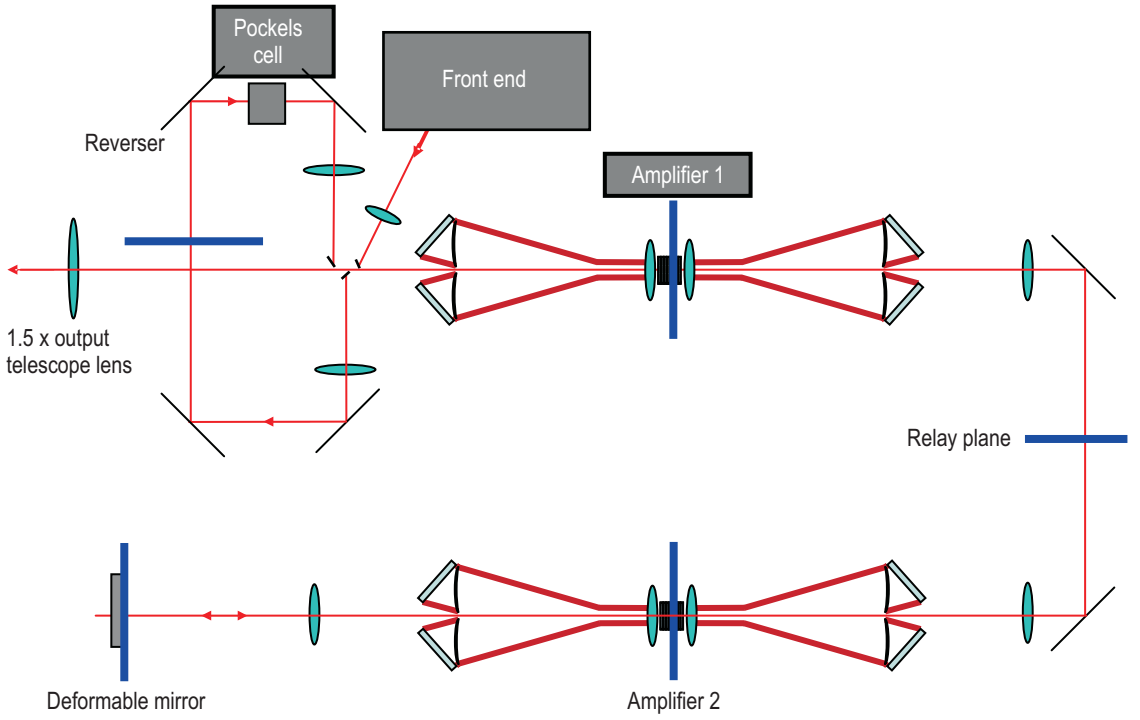

Fig. 8.31. Schematic of the Mercury laser at LLNL.

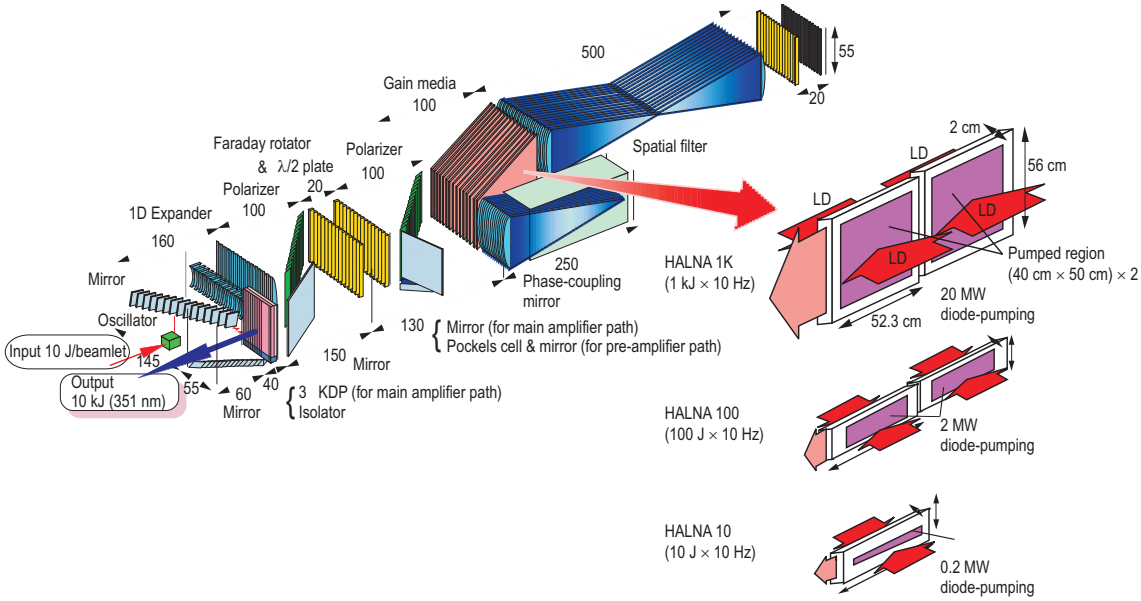

Fig. 8.32. The HALNA laser in Japan will demonstrate all the principles of the DPSSL for a full-sized IFE driver (kindly provided by Dr. T. Kawashima of ILE, Osaka University).

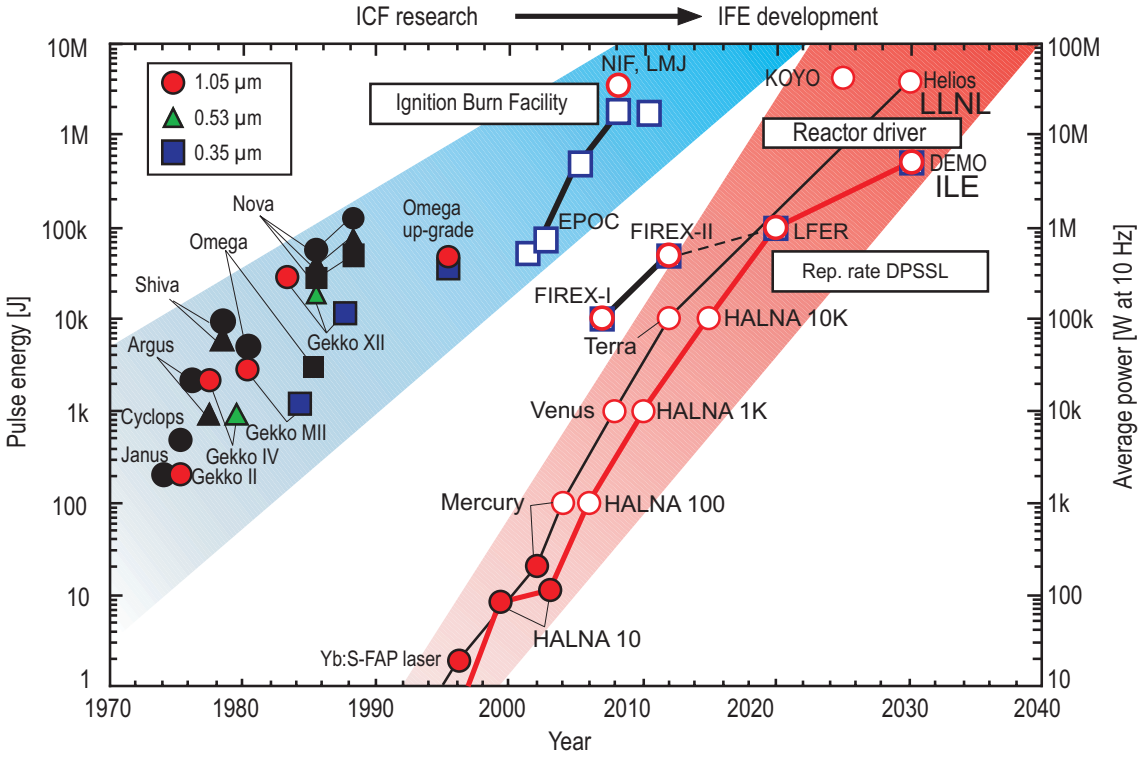

Fig. 8.33. Plans for developing DPSSL lasers for IFE are shown on a temporal chart that also shows past developments of solid-state research lasers through the ignition of targets on NIF and LMJ (kindly provided by Dr. T. Kawashima of ILE, Osaka University, and modified by the author).

8.4 Fast ignition lasers for laser-driven IFE

As discussed in Sect. 5.5.2, two drivers are needed for fast ignition. The first is a driver to compress the thermonuclear fuel capsule. The second is a short-pulse driver to ignite a small portion of the fuel as illustrated in Fig. 5.20. Only a few tens of kJ of energy is required but it must be delivered in about a picosecond. The power in the ignitor pulse will thus be $> 10^{15}$ W, or > 1 PW. If one tried to amplify a picosecond pulse to such high power, the pulse would damage the optical materials it traversed, including the lasing medium. However, a technique has been developed to produce such pulses. Called "chirped pulse amplification", the principle is to start with an initial short pulse and then use a pair of large aperture gratings to disperse the spectrum and thereby stretch the pulse in time by about a factor of 1000. The longer pulse is then amplified normally and a second pair of gratings is used to recompress the pulse to the picosecond timescale. The result is a PW pulse. A schematic of this laser architecture is shown in Fig. 8.34. This technique was demonstrated by using one beam of the Nova laser at LLNL to form such a PW beam.

The initial short pulse can be produced, for example, by a Ti-saphire laser. The initial short pulse is then amplified in a Nd:glass laser like that in Nova or NIF. In principle, either of the two laser types discussed above for the compression driver could also be made to produce a short, high-energy ignitor beam.

One critical issue for the ignitor laser is to make the final grating able to survive the high power of the compressed beam. The PW experiment on Nova required meter-scale gratings to do this. Figure 8.35 is a photograph of such a grating in the fabrication process.

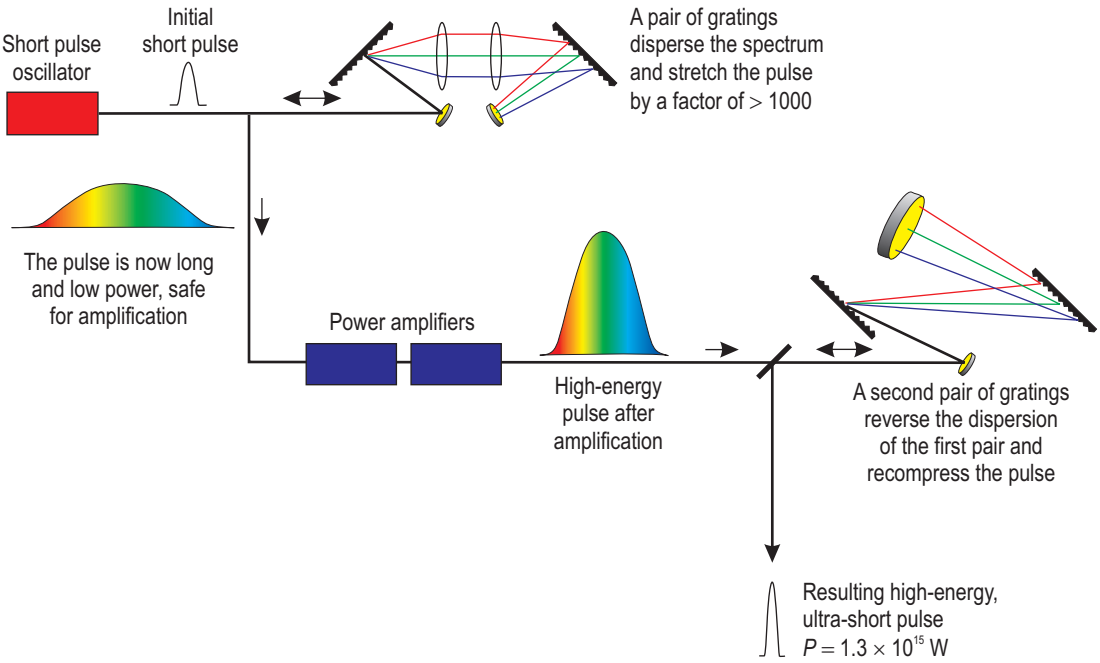

Fig. 8.34. Chirped pulse amplification permits production of PW laser beams.

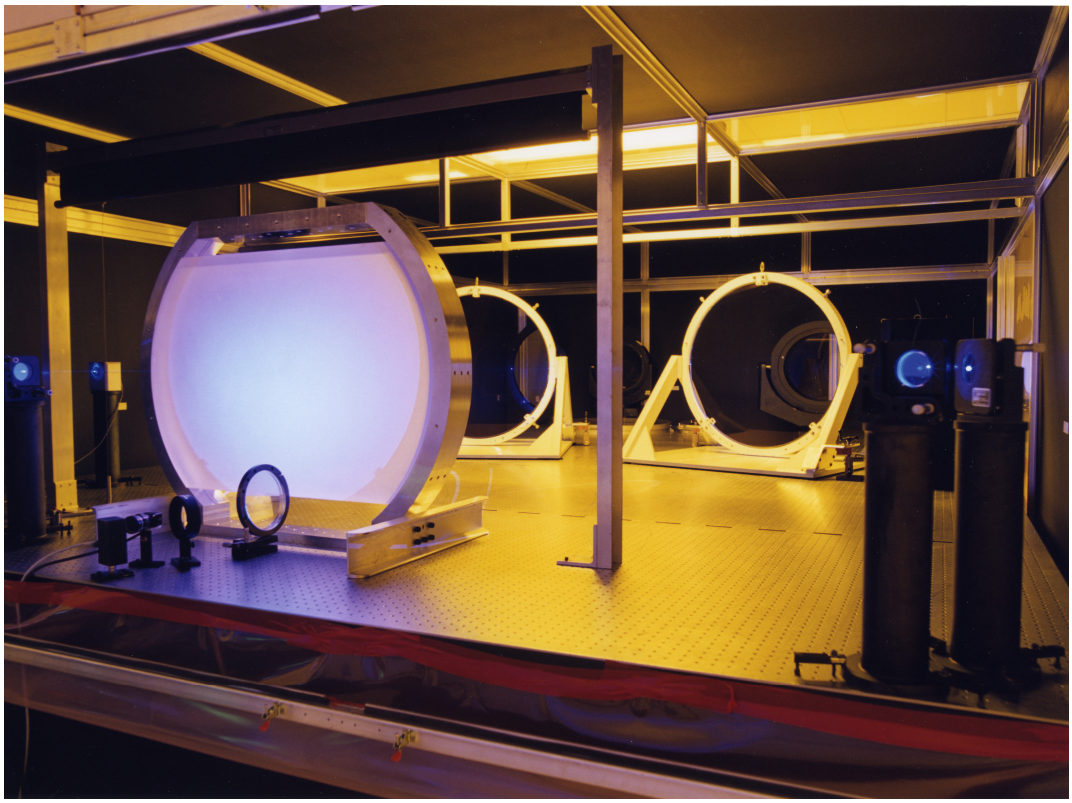

Fig. 8.35. The PW experiment on Nova required fabricating this 75 cm × 94 cm grating.

8.5 Reaction chamber and target positioning issues for laser IFE

As mentioned in Sect. 8.2, for central ignition targets, either directly or indirectly driven, the dry wall chamber is the current first choice in the United States. Section 5.5.5 outlined the features of the Sombrero dry-walled chamber concept that has been the subject of several IFE power plant studies [95Hog]. In this concept the chamber is made from a graphite fiber composite material. The first wall is protected by Xe gas. The density of the gas must be low enough that the focused laser beams do not break it down as they approach the target. The tritium breeding blanket consists of Li_2O granules entrained in a gas that flows through channels in the graphite structure. Figure 5.22 is a schematic of this chamber design. The figure shows a cross section of the chamber wall and the inlet and outlet pipes for the flowing Li_2O granules. The small circles in the figure are the entrance holes for the laser beams for symmetric illumination of direct drive targets. In Fig. 8.36 the 6.5 m inner radius Sombrero chamber is shown with two other reactor cores and with the NIF target chamber for comparison of scale. HYLIFE II, the thick liquid wall inertial fusion chamber is shown as well as the Westinghouse APWR 1300 fission reactor core. Other dry-walled chamber designs have a stationary Li bearing blanket through which gas flows to extract the tritium produced and are about the same size. As can be seen, the dry wall chamber is about twice the size of the HYLIFE II chamber and about three times that of the fission core. The dry wall chamber is simple in concept and in execution but there are some tough development issues.

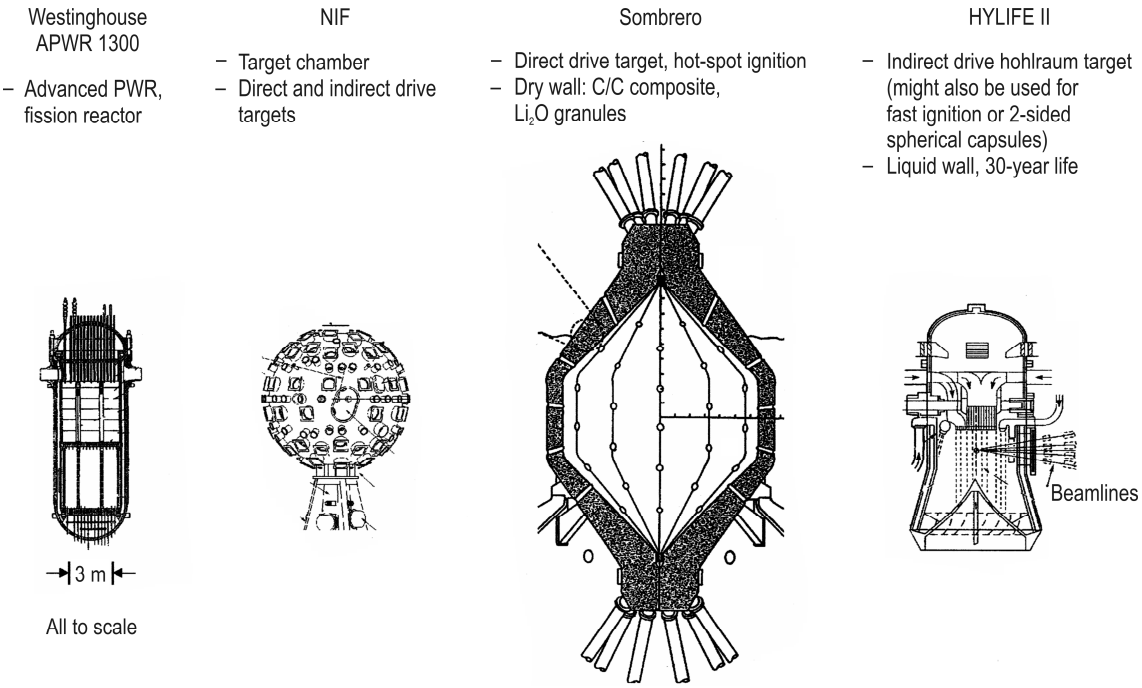

Fig. 8.36. A size comparison of the Sombrero dry wall chamber to a fission reactor core and to the HYLIFE II thick liquid wall chamber suitable for heavy ion driven targets. The NIF target chamber is also shown.

One of the issues for any dry wall chamber concept is the trade-off between wall survival and target survival during injection. Recent calculations of the output of a direct drive target [01Pet] suggest that almost 70 % of the energy exits the target as high-energy neutrons, almost 30 % is in the form of debris ions, mostly high-energy, and less than 1 % of the energy is emitted as X-rays.

Use of a background gas to protect the wall has been considered. One study [93Svi] found that 0.5 torr (67 Pa) of xenon gas was required in the chamber to prevent short-term damage from the ions to a composite graphite wall at 6.5 m radius. It was also found that the laser beams would not break down in this density of xenon gas. However, wall temperatures reached 1950 K, and stresses in the wall reached

50 MPa. It was estimated that such a wall might have to be replaced every 2…3 years. Research now is on developing advanced wall materials that will not suffer as much from the cyclic thermo-mechanical fatigue and the long-term agglomeration of helium bubbles. One promising approach is to use a tungsten armor bonded to a low-activation steel base. The tungsten would be micro-engineered into a foam or fibrous topology to relieve the stresses and to prevent helium entrapment.

There are three phenomena that limit the density of chamber gas that can be used: (1) survival of the target during injection, (2) tracking the target in the chamber, and (3) high-fidelity propagation of the laser beams to the target. Calculations of direct drive target survival for target designs shown in Fig. 8.7 were done to account for the radiative heat transfer from the walls and heat transfer due to condensation of background gas on the capsule during transit of the chamber. These calculations [03Raf] showed that the DT inside the capsule would receive 4…12 W/cm^2 from condensation of the Xe alone, even with a xenon pressure of only 50 mtorr. For the direct drive targets shown in Fig. 8.7, less than 1 W/cm^2 raises the fuel to its triple point. Clearly some protection for the DT fuel in the direct drive capsule is required. The capsule will have a sabot to protect it during its acceleration in the injector. However, if the sabot is left on during the chamber transit, it would be difficult to shed the sabot near the center in such a way as to guarantee that sabot parts do not interfere with one or more of the many laser beam lines. Therefore, it is generally assumed that any sabot will be shed before the capsule enters the chamber. To protect the target during transit of the chamber the design on the target itself will have to be changed. Recent results [03Raf] indicate that several alterations could ensure survival of the target. First, the initial temperature of the target can be lowered below the triple point as far as is consistent with target physics. Next, the target can have a dense plastic overcoat, followed by about 100 μm of an insulating foam, and, finally, the Au or Pd outer reflecting layer.

The temperature of the outer surface of the frozen DT in the target should not exceed the triple point of solid DT (19.79 K). Experiments have shown that smooth DT ice layers can be formed over foam layers at temperatures at least as low as 16 K. Thus the target outer surface can warm up 3.79 K before the outer surface starts to melt. The allowable heat flux on the target depends on the injection velocity and gas density. For example, assuming the target is in the chamber for 16 ms (corresponding to a 6.5 m radius chamber and a 400 m/s injection velocity), the allowable heat flux on a target starting at 16 K is 1.4 W/cm^2. If the chamber wall is at 1000 K, the radiation heating from the wall is about 0.2 W/cm^2. To stay below the 1.4 W/cm^2 total, the gas pressure should be below 15 mtorr (assuming the gas temperature is at the wall temperature). A 250 mg/cm^3 foam coating outside the target can provide additional thermal insulation. Calculations on this target suggest the gas pressure could be 5 to 8 times higher.

The target must be tracked as it traverses the chamber and the laser beams steered onto the target. Gas in the chamber is turbulent and perturbs the path of the target. Target designers require a +/−20 μm pointing accuracy for the compression lasers on the target. Modeling of the target movements through a gas shows that gas pressure should be below about 75 mtorr. Finally, the limit on gas density to allow propagation of the drive beams has been examined by several groups [03Set2] and found not to be the limiting factor on gas density.

Some alternative chamber designs are being considered to get around this dilemma. In the United States researchers are considering adding a 5 T magnetic field to divert the ions. KOYO is an alternative chamber design for direct drive being considered by researchers in Japan [04Nak]. They conceive flowing a thin layer of liquid lithium down the inner surface of the chamber wall to protect it from the X-rays and debris ions. This indeed will eliminate the damage to the first wall but introduces the complication of keeping the entire surface of the chamber coated with the liquid while providing for the large number of openings for the direct drive laser beams.

With the increased interest in fast ignition, consideration of power plant issues with cone focus fast ignition targets has begun [04Hog]. Chambers using direct drive cone targets would look much like those for central ignition targets because the illumination geometry for the compression laser would be similar. However, for cone focus indirectly driven targets, a different, and potentially more attractive possibility must be considered. Since the capsule compression for these targets does not have as stringent requirements on symmetry, it may be possible to use the HYLIFE II type of reaction chamber with these targets. This chamber was described in Sect. 5.5.5 and shown in Fig. 5.23. The first structural wall is protected from the target output by a thick layer of Li-bearing liquid like FLIBE. The advantage of this chamber is

that the structural wall can be made of well-understood materials (like certain steels) and still last the lifetime of the plant and be low in residual radioactivity. Figure 8.37a shows that about 0.5 m of molten salt would allow the wall to last the lifetime of the plant [96Sah], and Fig. 8.37b shows that a little thicker liquid flow would permit shallow burial of all waste [94Lee]. Use of the HYLIFE II concept may also eliminate the need for a 14 MeV neutron fusion materials development facility since the lifetime of the steel wall could be determined in existing neutron facilities.

The indirect drive cone focus targets do not have the target survivability issue of the direct drive targets because the hohlraum protects the fuel capsule during transit of the chamber. However, use of the HYLIFE II chamber concept requires that both the compression and the ignitor beams subtend small solid angles collectively. The target shown in Fig. 8.8b has the compression beams coming from one direction and the ignitor beams coming from the other. It is not yet known whether the solid angle required for either the compression or the ignitor beams will be sufficiently small that this concept can be used. As above, detailed self-consistent target calculations and some experiments will be needed to determine if the fast ignition cone targets can take advantage of the benefits of this chamber concept.

The general approaches and issues discussed in Sect. 5.5.4 for target fabrication and positioning systems apply to the laser targets discussed in this section. There are no additional issues for the target factory that are unique to laser targets. The target factory for an inertial fusion power plant will look and cost much the same for any driver, even though some of the equipment inside will be different and some of the materials used will be different. Therefore, this chapter will not consider target fabrication further.

A few words are required about target positioning. It has long been recognized that the simplicity and isotropy of the central ignition direct drive target would make target positioning much easier. The targets are one-dimensional and, therefore, there is no question about maintaining a necessary orientation during injection as with indirect drive targets. The issues discussed above concerning target survivability during injection cause more layers to be added but still the target is one-dimensional.

Cone focus fast ignition targets, however, whether they be direct or indirect, must maintain an orientation during injection. Fortunately, experiments on hohlraum targets [98Pet] indicate that if the targets are spun up to 200 revolutions per second, they will maintain their orientation during injection. Cone focus indirect drive targets will certainly be injected as easily as central ignition hohlraum targets (using any driver). However, it is envisioned that cone focus direct drive targets will be spun up and injected with the open end of the cone going first. This orientation helps protect the target from heating during injection. On the other hand this orientation during injection is aerodynamically unstable. Since the angle at injection will not be perfectly aligned, the axis of the spinning target will precess about the direction of travel. Aerodynamic drag will place non-symmetric loads on the cone and capsule. These will have to be calculated to determine if the target is survivable.

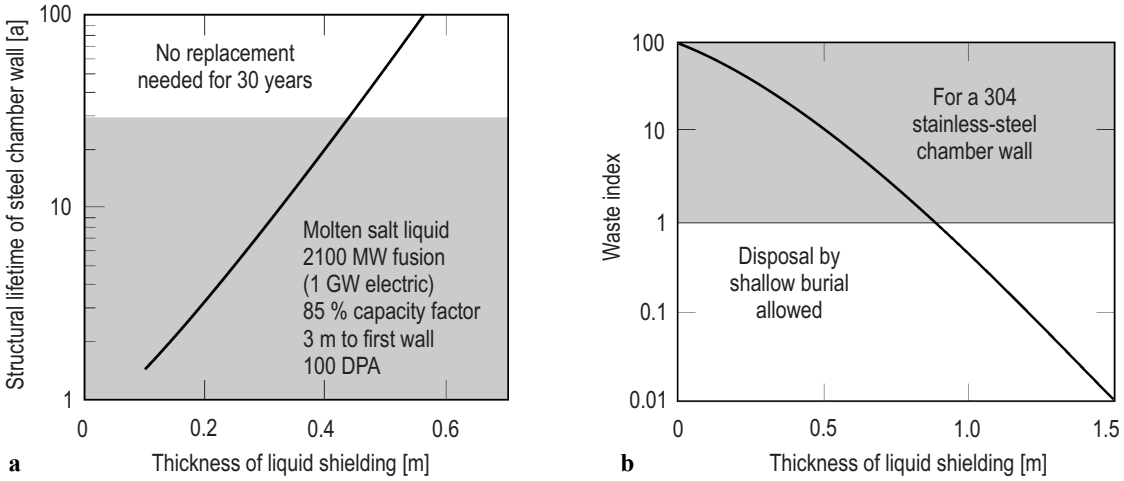

Fig. 8.37. Fast ignition power plants using cone focus indirect drive targets may be able to use thick renewable liquid flows for long life, low radioactivity and low maintenance.

Finally, one must consider the fate of a target that does not ignite. It is expected that targets will occasionally not ignite for a variety of reasons. The loss of fusion energy can easily be compensated for by increasing the yield or repetition rate slightly. However, in considering the fate of the dud target itself there are additional issues to resolve. The central ignition direct drive target has little mass so it will all be vaporized by the impinging laser beams even if the target does not ignite. The resulting low-temperature plasma debris isotropically expanding should pose no problem.

The story may be different for fast ignition targets. The cone focus targets are heavy, and the dense material may not completely vaporize. If it does not, then the expanding plasma may accelerate shrapnel to high velocity, and the damage that this shrapnel may produce on the wall or final optics must be considered [04Hog]. The cone focus hohlraum target will distribute any shrapnel produced uniformly. However, the cone focus direct drive target has the mass on one side. Therefore the expanding plasma from the compression lasers will accelerate pieces of the cone in the direction of the ignitor beam final optics. This issue needs further examination to determine if it can be resolved.

8.6 Final optics issues for laser IFE

One significant issue for inertial fusion is to determine how to get the driver beams into the fusion chamber and at the same time protect any high-value final beam processing elements that must be near the target from damage caused by the explosion of the target [95Hog]. For most drivers there must be beam steering, focusing, and/or channeling elements located as close to the target as possible. For lasers there must be a focusing element and for DPSSLs there will also be frequency conversion crystals to reduce the wavelength. Studies of laser-plasma interactions have found that instabilities can be deleterious to the target unless the wavelength of the laser is below about 0.5 μm. The KrF is naturally at about half this wavelength while the DPSSL is naturally at 1.06 μm. Thus in solid state lasers the frequency is tripled by putting the beams through first a potassium dihydrogen phosphate (KDP) crystal and then a crystal that is the deuterated version, KD*P. The resulting beam wavelength is 354 nm. Figure 8.38 shows that this frequency conversion can be done with almost 80 % efficiency. These results were obtained in the frequency conversion system used on NIF [94NIF].

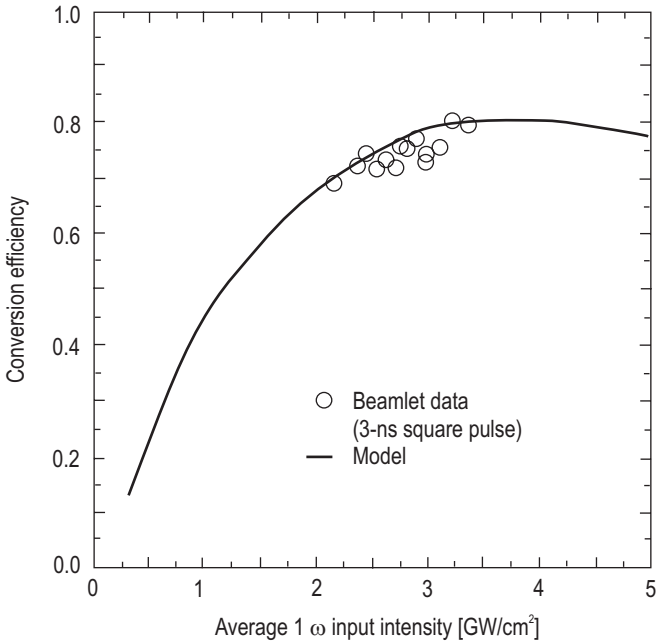

Fig. 8.38. Wavelength conversion from 1.0 μm to 354 nm can be done with about 80 % efficiency for high-intensity beams.

Since the frequency conversion process is not 100 % efficient, some unconverted 1 μm and 0.5 μm light (the first crystal doubles the frequency) must be diverted from hitting the target. This is done with a wedge or a diffractive optics plate. Since the laser-induced damage threshold in optical elements is lower for lower wavelength beams (an issue for KrF lasers), the DPSSL designers want to put these systems as close to the target as possible. For either type of laser driver, it is desirable to place the focusing element close to the target because it is easier to obtain the small spot sizes if the focusing lens is close. Since these final optical elements are relatively expensive it is necessary to protect them from the damaging effects of the exploding targets so that they will survive for many pulses. The final optics assembly of a solid state laser in a target research facility (like NIF) would, therefore, contain all the elements shown in Fig. 8.39. In addition there would have to be an optically clear vacuum barrier between the chamber, which must be operated at near vacuum, and the laser beam that will be near atmospheric pressure. Often, one of the existing elements is used for this vacuum seal. The KrF laser would not require the frequency conversion or color separation elements, but the rest of the final optics would be similar to those of a DPSSL laser.

Since the DPSSL laser beams are large (those on NIF have a 40 cm × 40 cm aperture, but the DPSSL beams will be somewhat smaller than this), large crystals must be grown. This was needed for Nova and NIF flashlamp-pumped Nd:glass lasers as well. For Nova growth of the conversion crystal boules took 1…2 years. For NIF, a new fast growth method was developed resulting in the ability to grow the 45-cm boule shown in Fig. 8.40 in only one month. This lowered the cost and greatly helped the NIF construction schedule [04Mos].

For a laser-driven fusion power plant there is an additional damage issue to consider. Neutrons impinging upon optical elements cause the formation of "color centers" that reduce their transmission capability. Therefore another optical system is needed to deflect the beam in a "dogleg" fashion so that the high-cost final optical elements do not directly see the neutrons from the exploding targets [01Lat]. The resulting geometry is shown in Fig. 8.41.

The "dogleg" design consists of bending the laser beams twice after the high-value optics. First, to move the beam into a line of sight to the target, and second, to make the beam move parallel to that line of sight. Thus, no matter how much maneuvering is done, there will be one optical element that will have a direct line of sight to the target. There may be a gas-filled tube to stop the X-rays and debris, and/or a fast closing shutter. However, the neutrons will get through and they must be disposed of in a radiation dump after traversing the final optics. These final optics may be refracting, reflecting or diffracting, and all have been considered.

Wedges bend light through refraction, are well understood and are relatively inexpensive to fabricate. A single wedge is being used in NIF to separate colors as described above. When neutrons impinge upon optical material like fused silica (SiO_2), the displacement of atoms causes "color centers" to form which tend to absorb or scatter light. Eventually the optics will not pass enough of the laser beam for target ignition. However, it has been found that thermal annealing will cause many of the color centers to heal and the optics will become transparent again [95Hog]. Figure 8.42 describes the processes and types of color centers that form, as well as the effect of annealing [01Lat].

As noted in Fig. 8.42 the different color centers absorb at different wavelengths. The annealing process is more effective for certain types of color center than others. The result is shown in Fig. 8.43. An SiO_2 sample was heated to 105 °C and irradiated with 10^{11} rad of neutrons at the LANSCE facility at Los Alamos (this dose is equivalent to about 0.4 full power years (FPY) in an IFE power plant). It was then annealed for various times at 380 °C. As can be seen, the optical density increases for all wavelengths shorter than 700 nm but annealing causes the optical density to return to normal for wavelengths greater than 350 nm. This seemed to indicate that wedges might work well for DPSSLs but not for KrF lasers. It also suggested that if the optics were operated at an elevated temperature, perhaps the annealing could occur "on line".

Figure 8.44 shows the result of a dose of $\approx 10^{11}$ rad neutrons upon an SiO_2 sample held at 426 °C. The figure shows that, at this temperature, color centers do not increase absorption for wavelengths greater than 350 nm. It also shows that the color center effects and shorter wavelengths can be eliminated by further annealing at 600 °C. However, light scattering may reduce the transparency and, therefore, limit the thickness of fused silica that can be used [01Lat].

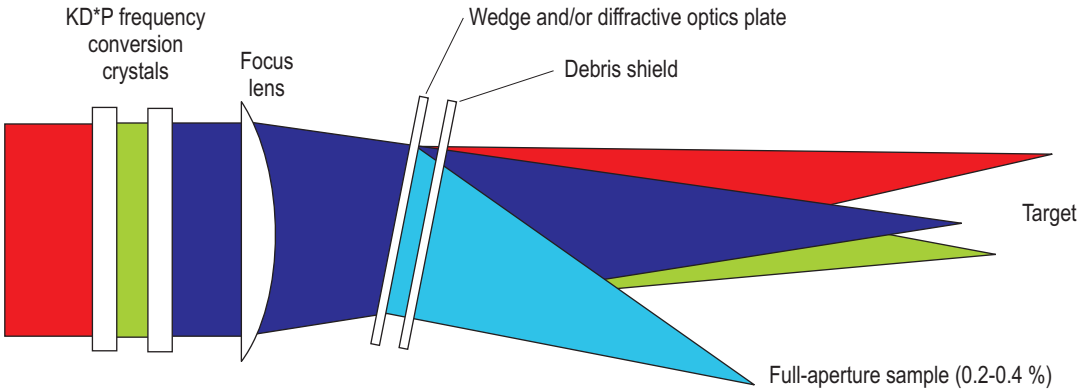

Fig. 8.39. The final optics for a solid state laser such as the one in NIF must contain frequency conversion, focusing, color separation, smoothing, and debris protection.

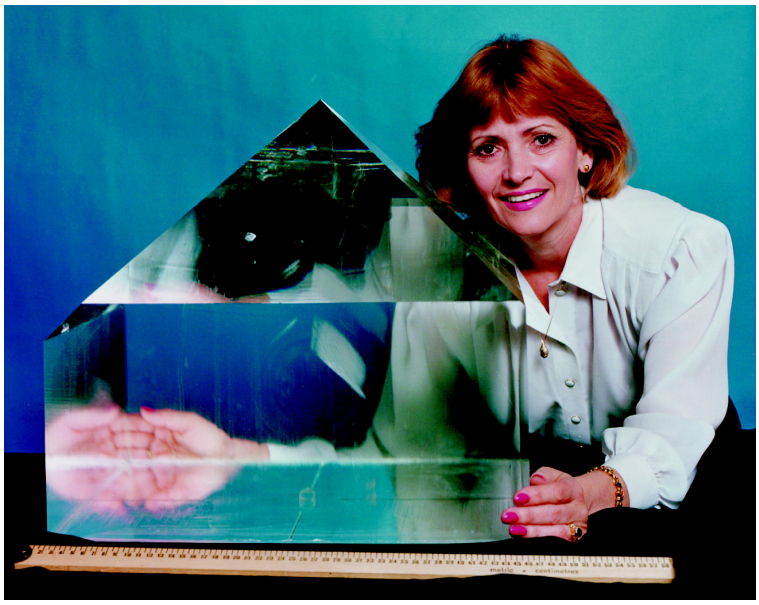

Fig. 8.40. Many 45-cm KDP crystal boules were grown for the NIF laser.

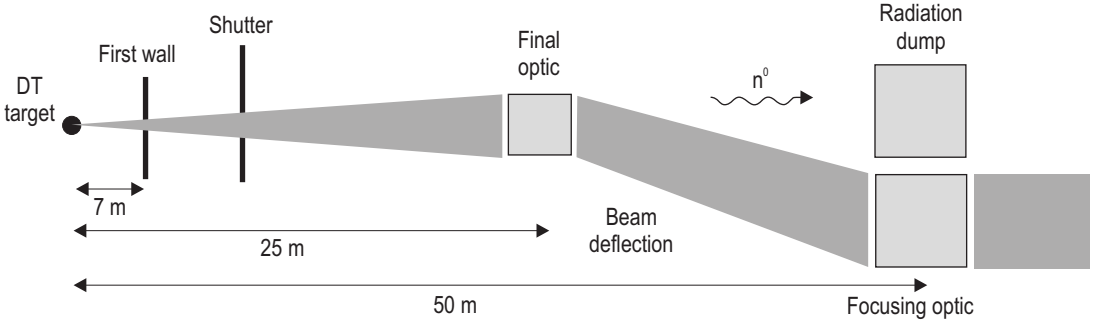

Fig. 8.41. The laser beams must "dogleg" into their path to the target to avoid neutron damage.

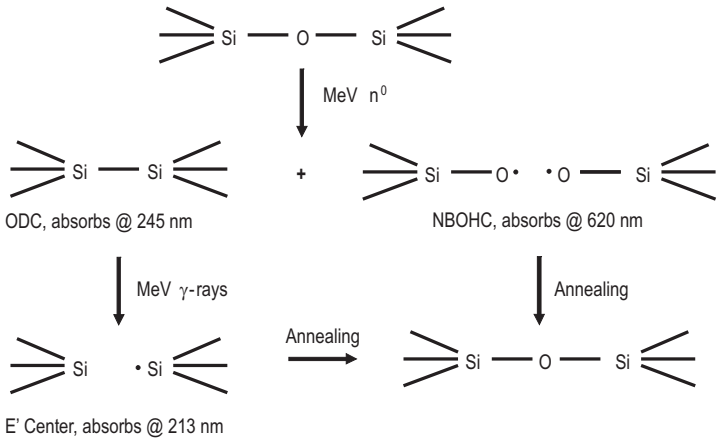

Fig. 8.42. Neutron irradiation leads to the formation of color centers in SiO_2, but annealing can restore the transparency.

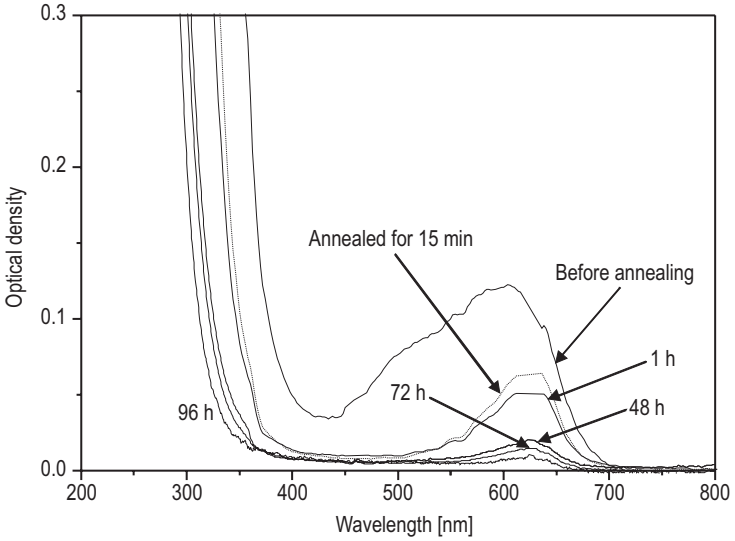

Fig. 8.43. Following a neutron dose of $\approx 10^{11}$ rad with the sample at 105 °C, the samples are annealed at 380 °C for the times indicated [01Lat].

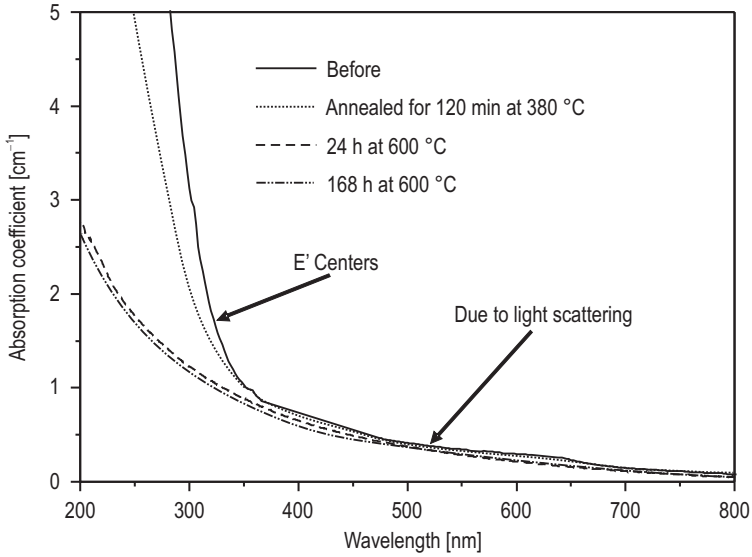

Fig. 8.44. Absorption coefficient in SiO_2 operated at 426 °C with a dose of $\approx 10^{11}$ rad neutrons.

The potential limit on the thickness of the transmitting optics suggested that perhaps diffractive optics would be a better choice. The absorption coefficient of 1 cm^{-1} at 350 nm would result in 90 % transmission for a 1 mm thick optics. Therefore, perhaps a diffractive grating could be used to deflect the beam into the line of sight. Such a grating could also provide the color separation needed for DPSSLs. Large-aperture SiO_2 diffractive optics have been constructed using the 2-mask lithographic process with HF etching bath. Figure 8.45a shows an 80 cm diameter, 1 mm thick fused silica Fresnel lens. This lens has tabs along several radii to allow folding for transport into space. However, the fabrication technique could also result in a monolithic lens of the same size. The fact that a lens was produced also indicates that the final optics might be used as the focusing element as well, although an off-axis Fresnel lens would be required to simultaneously steer the beam into the line of sight [01Lat]. A 5 m diameter array of such lenses as shown in Fig. 8.45b may allow placing the ignitor beams for a FI target far enough away to survive the target explosion

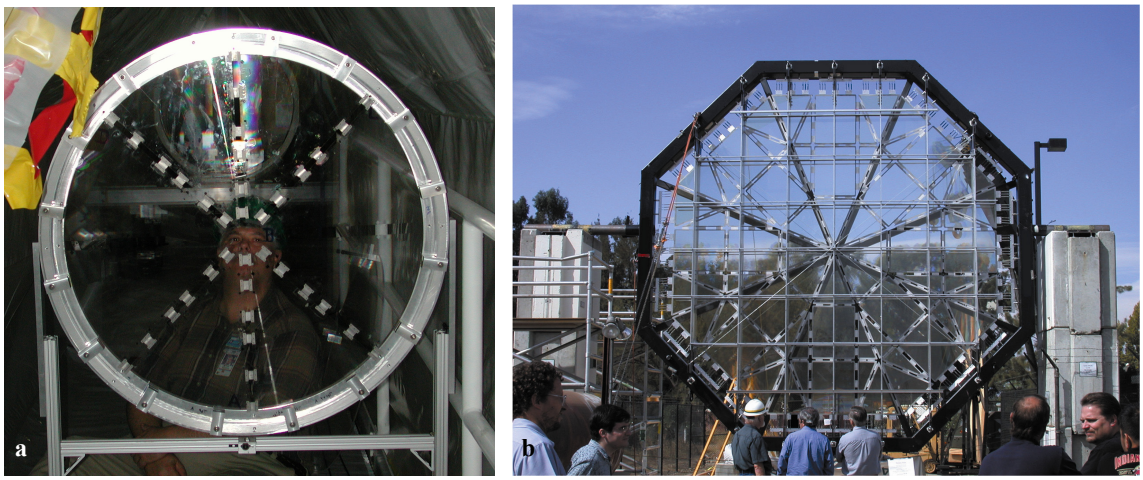

Fig. 8.45. **(a)** An 80 cm diameter, 1 mm thick Fresnel lens was fabricated in the Eyeglass project at LLNL. **(b)** An even larger Fresnel lens array (5 m diameter) was later fabricated.

The third alternative under investigation is the grazing incidence metal mirror (GIMM). Any mirror in the target line of sight will be degraded by neutron swelling and He bubble production. Both will distort the surface of the mirror. The effects can be reduced by moving the mirror further away or by tilting the mirror to a grazing incidence (< 10°). Most mirrors are made by coating the backside of a pane of glass with a reflecting metal. However, in the case of the laser final optics the metal should be placed on the front side of the substrate so that the laser beam does not go through any material. Figure 8.46 shows the reflectivity of several metal surfaces as a function of wavelength [01Til]. Clearly Al is of most interest for wavelengths of either the KrF or DPSSL lasers. Figure 8.47 shows the reflectivity as a function of angle of incidence for various thicknesses of sputtered Al 1101. A reflectivity of more than 92 % can be maintained if the Al thickness is 50 nm or greater [01Til]. The damage resistance (to laser light) of these types of metal mirrors has been measured to be > 20 J/cm^2 for 351 nm light, and > 8 J/cm^2 for 248 nm light, which is much greater than the 5 J/cm^2 needed. The resistance to damage from target emissions and any protection necessary has not been established.

For central ignition direct drive targets these final optics must be placed in a symmetric pattern illuminating the target from all directions. Figure 8.48 shows one such resulting arrangement. To arrange all the beams in the proper illumination geometry and place the GIMMS and neutron dumps at a reasonable distance from the target requires a cubical building about 100 m on a side.

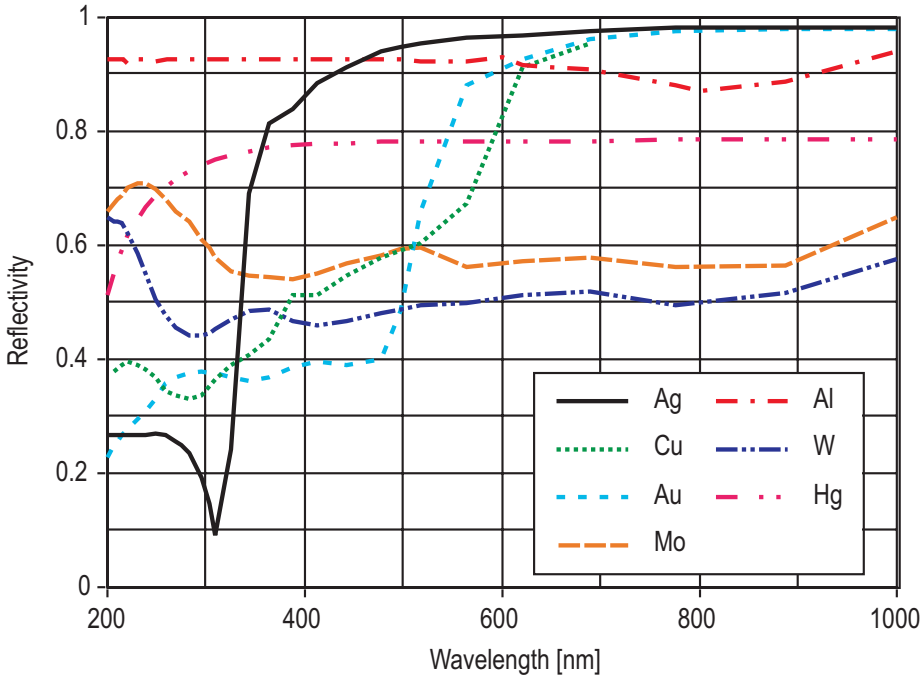

Fig. 8.46. Reflectivity at normal incidence of several polished metal surfaces [01Til].

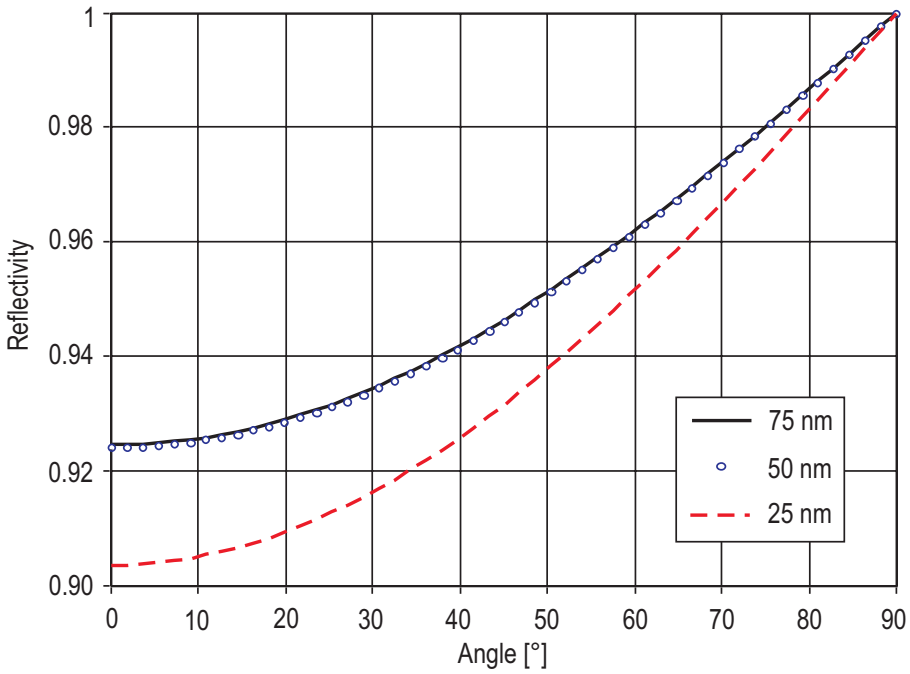

Fig. 8.47. Reflectivity versus angle of incidence for sputtered Al 1101 of various thicknesses [01Til].

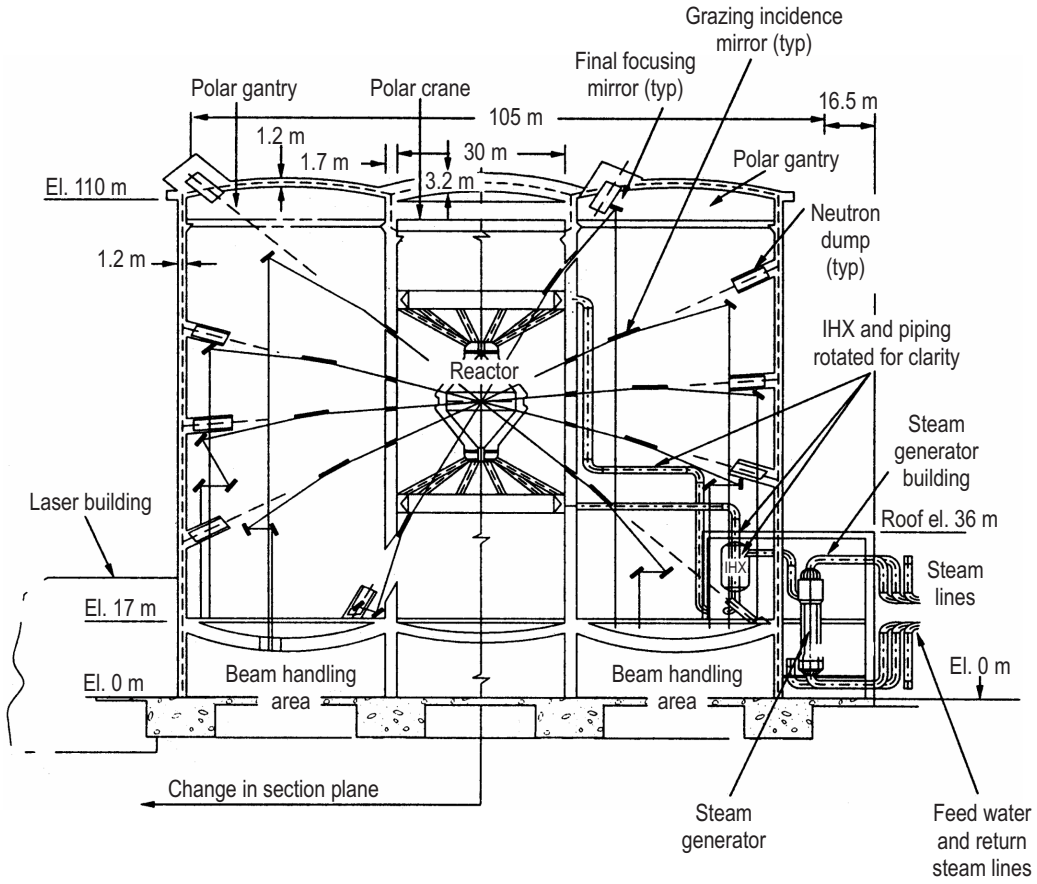

Fig. 8.48. Reaction chamber and final optics require a large reactor building in the Sombrero design.

Figure 8.48 shows another potential advantage of the fast ignition concept using cone focus targets. If the symmetry requirements can be relaxed as discussed in Sect. 8.5 above, then the beams could be clustered into a smaller total solid angle. Thus, while the building might be 100 m long, it need not be 100 m wide and 100 m tall. Determining the size needed will require detailed target calculations on how much the symmetry requirements can be relaxed.

The final optics for the ignitor beams pose a different issue. The ignitor beams have very high intensity and must be focused to a smaller spot than the compression beams to ignite a small portion of the fuel on the edge of the compressed target. In general to obtain the small spot size would suggest moving the final focusing optics closer to the target. However, for survivability we would like to move them further away. It has been calculated [02Mim] that the cones should produce some focusing effect on the laser beams and, thus, the focus spot of the laser itself may not have to be as small as the final ignition spot size. The large aperture diffractive optics discussed above may offer promise. If a good-quality large diffractive optics can be produced, perhaps it can be large enough and far away enough that it will survive both the high-intensity ignitor beams and focus to a small enough spot that the cone target can ignite. A self-consistent final optics design for fast ignition targets has not yet been determined.

8.7 Development path for laser IFE

The development of laser fusion has been proceeding in a series of facilities of increasing size as illustrated in Fig. 8.1 of this chapter. In the last several years, the MFE and IFE communities in the United States have agreed to a common set of descriptors for the remaining few stages of fusion energy development. These are illustrated in Fig. 8.49. Four stages of R&D are defined: (1) concept exploration, (2) proof of principle, (3) performance extension, and (4) fusion energy development. The stages are defined by the level of funding required and the degree of integration of subsystems into systems and whole power plant demonstrations. The various advocates of one or other concept will disagree about how far along their concept is and when the division between stages will occur. However, each has defined the set of "demonstrations" their concept must perform in order to move between stages. The particular vision of the "road map" for IFE development in Fig. 8.49 shows current development of KrF and DPSSL lasers as being in the "proof of principle" stage [99Cam]. At this stage demonstrations of driver performance, from power supply to focused spot in a target chamber, in a design that can scale to a power plant sized module are the main ingredients. One of the features of IFE is that the target ignition programs in France and the U.S. are being paid for by the respective weapons programs. The NIF and LMJ facilities are two-billion-dollar facilities that will demonstrate target ignition and propagating burn for all targets regardless of driver type. Therefore, what remains is for each driver to prove that it can obtain the required intensity inside a target that it could generate the ignition conditions that NIF and LMJ will demonstrate. The separate driver programs must also demonstrate driver qualities like repetition rate, intensity, efficiency, etc. In parallel with these developments, power plant technology is being examined to assure that there are no road blocks to IFE if the targets and drivers perform as projected, and to assure that each research facility will perform as expected.

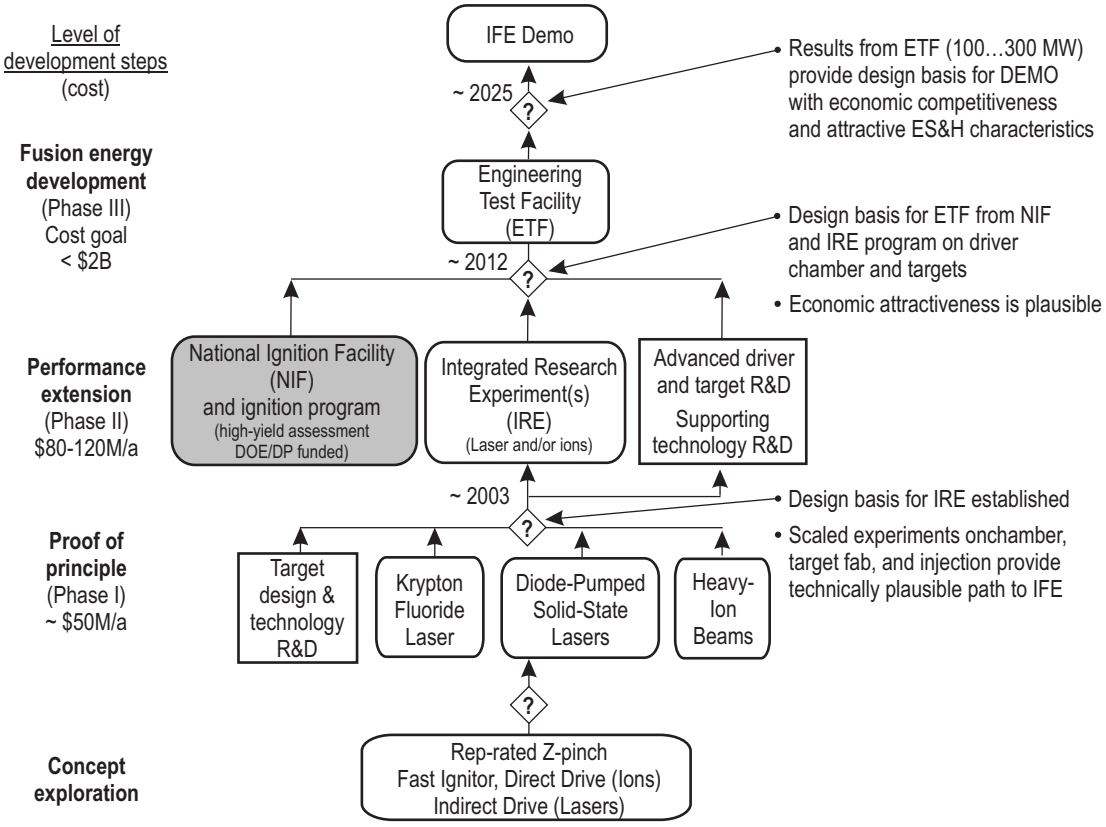

Fig. 8.49. One possible development path for laser fusion.

After a driver has demonstrated fundamental feasibility, it must demonstrate integrated performance in a reactor-scale module. This step is called an Integrated Research Experiment (IRE). Both KrF and DPSSL lasers have designed their concepts for what an IRE based upon their driver would look like. Building and operating an IRE would cost in the range of $100 M per year. The principle is that the IRE module could be replicated to build the full-sized ETF or power plant driver. While the IRE driver would not be large enough to ignite a target it would have demonstrated full driver performance in the scalable module and would demonstrate target injection, tracking and bringing the driver beams to the target.

The final stage before a demo is called the Engineering Test Facility. In this facility a full-sized power plant driver would demonstrate the full target gain required for a power plant. In addition, with the driver running at reduced pulse energy but at full repetition rate, the ETF would demonstrate igniting targets at the required repetition rate. These two separate goals for the ETF represent a nice feature of IFE. The fusion power produced in an IFE plant is the product of the yield of each target times the repetition rate. The two can be varied independently. The advantage of doing so is that a high repetition rate demonstration with lower-yield targets can be done in a scaled-down chamber at a lower average power level. A demonstration of full repetition rate might take place in a chamber generating only, perhaps, ≈ 100 MW of thermal power instead of the 3000 MW required in a full-scale "demo". This approach is less expensive than operating at full power and, thus, several reactor chambers can be tested to determine the best concept. After the best chamber and other system components are demonstrated, a full-sized chamber can be built using the same driver. The ETF can become the "demo" without an additional large-scale construction project. The demo would operate at full power and demonstrate the reliability and economic viability of the entire IFE plant.

What is not shown in Fig. 8.49 is a 14 MeV neutron fusion materials development facility. For most IFE power plant concepts, this facility would be required to determine the lifetime of the structural components in the presence of the damaging effects of the fusion output. However if the thick liquid wall HYLIFE II chamber concept can be used, as perhaps for the laser fast ignition indirect drive target, the neutrons and other damaging output is so moderated by the time it reaches the structural wall that existing neutron sources may be used to examine material lifetimes. Eliminating the need for a special materials development facility could lower the cost and shorten the time for development for these options.

The separability of the driver, chamber and target factory in IFE makes it possible to develop various parts of an IFE system at different locations. Research organizations around the world are working on many concepts for various subsystems. International cooperation and collaboration through such organizations as the IAEA can be a very effective way to stimulate missing research and multiply the benefits of each organization's efforts.

Acknowledgements

The author would like to thank many colleagues for their informative discussions and advice and for their generosity in allowing him to use their facts, figures and sometimes even their words in this chapter. In particular, Dr. John Sethian of the Naval Research Laboratory was particularly helpful and generous in providing his information and many figures and manuscripts for use in the section on KrF lasers. Indeed most of what is there is from the work of Dr. Sethian and his colleagues. I also thank Dr. Sethian for providing access to the meetings of the High Average Power Laser Program, which he leads. This very active program is developing the science and technology of all aspects of laser fusion power plant development with central ignition, direct drive targets. Several of the references are to the website on which all talks at these meetings are published shortly after each meeting. This near real time access to current research proved invaluable for several of the sections of this chapter.

For the material on DPSSL laser development at LLNL, the author is indebted to Dr. Stephen Payne and Dr. Camille Bibeau of LLNL for discussions and access to their recent facts, figures, presentations and manuscripts. Dr. Payne and Dr. Sethian helped the author by proofreading his material and offering many helpful suggestions and corrections. The author also thanks Prof. Sadao Nakai from ILE in Osaka, Japan, and from the Kochi National College of Technology for proofreading and providing helpful information. Prof. Kunioki Mima of ILE provided many helpful discussions and ideas over many years, and

Dr. Toshiyuki Kawashima provided current figures of the DPSSL program in Japan. The author was a Visiting Professor at ILE for three months in 2002. Many colleagues at ILE provided valuable insight to their approach to DPSSL lasers and cone focus targets during his tenure in Japan.

The author would also like to thank his colleagues in the Fusion Energy Program at LLNL for many helpful discussions and for access to their work and publications.

The overriding view of the development path for inertial fusion was developed by the author in collaboration with 87 other researchers in assembling Energy from Inertial Fusion [95Hog]. This book was produced by the International Atomic Energy Agency (IAEA) in Vienna, Austria, under the guidance of the International Advisory Committee on Inertial Fusion Energy, of which the author was Chair. The author also served as Scientific Editor of this work and gained much insight into research directions in all parts of the world on inertial fusion. The author is in debt to the IAEA for the opportunity to help produce this broad look at inertial fusion energy.

8.8 References for 8

64Bas Basov, N.G. et al: Conditions for heating up of a plasma by the radiation from an optical generator, Sov. Phys. – JETP **19** (1964) 123.

65Rig Rigrod, W.W.: Saturation Effects in High-Gain Lasers, Journal of Applied Physics **36** (1965) 2487.

72Nuc Nuckolls, J. et al.: Laser compression of matter to super-high densities: Thermonuclear (TN) applications, Nature (London) **239** (1972) 139.

80Ric Rice, J.K. et al.: Oscillator Performance and Energy Extraction from a KrF Laser Pumped by a High-Intensity Relativistic Electron Beam, IEEE Journal of Quantum Electronics, **QE-16**, 12 (1980) 1315.

84Kat Kato, Y. et al.: Random phasing of high power lasers for uniform target acceleration and plasma instability suppression, Phys. Rev. Lett. **53** (1984) 1057.

85CEL CEL-V Laser Research Group: Twenty-two years of laser-matter work at Centre D'etudes de Limeil-Valenton (CEL-V), Nucl. Fusion **25** (1985) 1333.

86Kau Kauffman, R.L.: X-ray Conversion Efficiency, 1986 LLNL Laser Program Unclassified Annual Report, UCRL-50021-86, Lawrence Livermore Natl. Lab., Livermore CA (1986).

87Leh1 Lehmberg, R.H., Goldhar, J.: Fusion Technology **11** (1987) 532.

87Leh2 Lehmberg, R.H. et al.: J. Appl. Phys. **62** (1987) 2680.

89Sku Skupsky, S. et al.: Improved laser beam uniformity using the angular dispersion of frequency modulated light, J. Appl. Phys. **66** (1989) 3456.

90Low Lowdermilk, W.H.: High energy lasers for inertial fusion research and applications, Resonances (M.D. Levenson et al., Eds.), World Scientific, Singapore (1990) 55.

92Bas Basov, N.G. et al.: Laser Driver for inertial confinement fusion, Drivers for Inertial Confinement Fusion (Proc. Tech. Comm. Mtg. Osaka, 1991), Inst. Of Laser Engineering, Osaka (1992) 13.

92Svi Sviatoslavsky, I.N. et al.: A KrF laser driven inertial fusion reactor, SOMBRERO, Fusion Tech. **21** (1992).

93Svi Sviatoslavsky, I.N. et al.: SIRIUS-P-A Symmetric Illumination Power Plant, Rep. UWFDM-950, Univ. of Wisconsin, Madison (1993).

94Lee Lee, J.D.: Waste Disposal Assessment of HYLIFE-II Structure, Fusion Technology **26** (1994) 74.

94NIF National Ignition Facility Conceptual Design Report, Rep. UCRL-PROP-117093, Lawrence Livermore Natl. Lab., Livermore CA (1994).

95Hog Hogan, W.J. (Scientific Editor): Energy from Inertial Fusion, IAEA, Vienna, Austria (1995).

95Kru Krupke, W., LLNL, private communication (1995).

95Pay Payne, S., LLNL, private communication (1995).

96Obe Obenschain, S.P. et al.: Phys. Plasmas **3** (1996) 2098.

96Sah Sahin, S. et al.: Radiation damage in liquid-protected first-wall materials for IFE-reactors, Fusion Technology **30** (1996) 1027-1035.
97Set Sethian, J.D. et al.: A Large Area Electron Beam Pumped Krypton Fluoride Laser Amplifier, Rev. Sci. Instrum. **68** (1997) 2357.
98Key Key, M. et al.: J. Fusion Energy **17** (1998) 3.
98Lin Lindl, J.D.: Inertial Fusion Energy, Springer-Verlag, New York (1998).
98Pet Petzoldt, R.: IFE Target Injection and Tracking Experiment, Fusion Technology **34** (Nov. 1998) 831.
99Cam Campbell, E.M., Hogan, W.J.: The National Ignition Facility—Applications for inertial fusion energy and high-energy density Science, Plasma Phys. Control. Fusion **41** (1999) B39-B56.
99Oku Okuda, I. et al.: Fusion Engineering and Design **44** (1999) 377.
00Bod Bodner, S.E. et al.: High Gain Direct Drive Target Design for Laser Fusion, Phys. of Plasmas **7**, (2000) 2298.
00Set Sethian, J.D. et al.: Pulsed Power for a Rep-Rate, Electron Beam Pumped KrF Laser, IEEE Trans. Plasma Sci. **28** (2000) 1333.
01Kod Kodama, R. et al.: Fast Heating of Ultrahigh-density Plasma as a Step Towards Laser Fusion Ignition, Nature **412**, 6849 (August 23, 2001) 798-802.
01Lat Latkowski, J.F. et al.: High Average Power Laser Program meeting Pleasanton CA, November 2001, URL: http://aries.ucsd.edu/HAPL/MEETINGS/0111-HAPL/program.html.
01Lu Lu, J. et al.: Appl. Phys. Lett. **78** (2001) 3586.
01Oku Okuda, I. et al.: Appl. Phys. B: Lasers Opt. **75** (2001) 623.
01Pay Payne, S. et al.: Progress report on the Mercury Laser, High Average Power Laser Program meeting Washington DC., June 1, 2001, URL: http://aries.ucsd.edu/LIB/MEETINGS/0105-NRL-LASER-DP/.
01Pet Peterson, R.R. et al.: High Average Power Laser Program meeting Washington DC., June 1, 2001, URL: http://aries.ucsd.edu/LIB/MEETINGS/0105-NRL-LASER-DP/.
01Til Tillack, M. et al.: High Average Power Laser Program meeting Washington DC., June 1, 2001, URL: http://aries.ucsd.edu/LIB/MEETINGS/0105-NRL-LASER-DP/.
01Zvo Zvorykin, V.D. et al.: Laser Part. Beams **19** (2001) 609.
02Heg Hegeler, F. et al.: Reduction of Edge Emission in Electron Beam Diodes, Physics of Plasmas **9** (2002) 4309.
02Mim Mima, K., ILE, private communication (2002).
02Set Sethian, J.D. et al.: Fusion Energy with Lasers, Direct Drive Targets and Dry Wall Chambers, IAEA Lyon meeting paper OV/3-2 (2002).
02Wan Wang, N. et al.: Laser Part. Beams **20** (2002) 119.
02Wei Weidenheimer, D. et al.: Advanced Pulsed Power Concept and Component Development for KrF Laser IFE, to be published in the Proceedings of the IEEE Power Modulator Conference, Hollywood, CA, June 31-July 2, 2002, IEEE Piscataway, NJ.
03Fri1 Friedman, M et al.: Eliminating the transit-time instability in large-area electron-beam diodes, App Physics Letters **83** (2003) 1539.
03Fri2 Friedman, M. et al.: Initiation and prevention of the Transit Time Instability, submitted for publication 2003.
03Nor Norimatsu, T. et al.: Update for the drag force on an injected pellet and target fabrication for inertial fusion, Fusion Sci. Technol. **43** (2003) 339-345.
03Raf Raffray, A.R. et al.: High Average Power Laser Program meeting Madison Wisc., Sept. 24-25, 2003, URL: http://aries.ucsd.edu/HAPL/MEETINGS/0309-HAPL/program.html and Alb. NM April 10, 2003, URL: http://aries.ucsd.edu/HAPL/MEETINGS/0304-HAPL/program.html.
03Set1 Sethian, J.D. et al.: Physics of Plasmas 10, 5 (2003) 2142.
03Set2 Sethian, J. et al.: Fusion Energy with Lasers, Direct Drive Targets, and Dry Wall Chambers, Nuclear Fusion **43** (2003) 1693-1709.

04Cav Cavailler, C. et al.: Status of the LMJ Project, to be published in Proceedings of the 3rd International Conference on Inertial Fusion Sciences and Applications (IFSA2003), American Nuclear Society (2004).

04Gle Glenzer, S. et al.: Progress in Long-Scalelength Laser Plasma Interactions, to be published in Proceedings of the 3rd International Conference on Inertial Fusion Sciences and Applications (IFSA2003), American Nuclear Society (2004).

04Heg Hegeler, F. et al.: Efficient Electron Beam Pumping of Repetitively Pulsed High Energy Krypton Fluoride Lasers, Proceedings of the 3rd International Conference on Inertial Fusion Sciences and Applications (IFSA2003), American Nuclear Society (2004).

04Hog Hogan, W.J., Meier, W.R.: Technology Issues and Benefits of a Fast Ignition Power Plant with Cone Targets, Proceedings of the 3rd International Conference on Inertial Fusion Sciences and Applications (IFSA2003), American Nuclear Society (2004).

04Mos Moses, E.: The National Ignition Facility: Transition to a Target Shooter, Proceedings of the 3rd International Conference on Inertial Fusion Sciences and Applications (IFSA2003), American Nuclear Society (2004).

04Nak Nakai, S., Mima, K.: Laser driven inertial fusion energy: present and prospective, Rep. Prog. Phys. **67** (2004) 1-29.

04Set Sethian, J.D. et al.: Development of Krypton Fluoride Lasers for Fusion Energy, Proceedings of the 3rd International Conference on Inertial Fusion Sciences and Applications (IFSA2003), American Nuclear Society (2004).

04Wol Wolford, M.F. et al.: Electra As An Oscillator: A Repetitively Pulsed, 500 J, 100 ns, KrF Laser, Proceedings of the 3rd International Conference on Inertial Fusion Sciences and Applications (IFSA2003), American Nuclear Society (2004).